Silence of the Fish: Injection of Photoswitchable Short Interfering RNA Oligonucleotides into Japanese Medaka Embryos *(Oryzias latipes)* to Photochemically Control Gene Silencing

by

Makenzie Mateus

A thesis submitted to the
School of Graduate and Postdoctoral Studies in partial
fulfillment of the requirements for the degree of

Master of Science

in

Applied Bioscience (Molecular Biology)

Faculty of Science

University of Ontario Institute of Technology (Ontario Tech University)

Oshawa, Ontario, Canada

December 2023

THESIS EXAMINATION INFORMATION

Submitted by: **Makenzie Mateus**

Master of Science in **Applied Bioscience (Molecular Biology)**

Thesis title: Silence of the Fish: Injection of Photoswitchable Short Interfering RNA Oligonucleotides into Japanese Medaka Embryos *(Oryzias latipes)* to Photochemically Control Gene Silencing

An oral defense of this thesis took place on December 8, 2023, in front of the following examining committee:

Examining Committee:

Chair of Examining Committee	Dr. Dario Bonetta
Research Supervisor	Dr. Jean Paul Desauniers
Research Co-supervisor	Dr. Denina Simmons
Examining Committee Member	Dr. Sean Forrester
Thesis Examiner	Dr. Shilpa Dogra

The above committee determined that the thesis is acceptable in form and content and that a satisfactory knowledge of the field covered by the thesis was demonstrated by the candidate during an oral examination. A signed copy of the Certificate of Approval is available from the School of Graduate and Postdoctoral Studies.

ABSTRACT

The siRNA duplex functions by binding to and cleaving mRNA, a process known as the RNAi pathway. Existing siRNAs face challenges such as off-target effects and unpredictable prolonged gene-silencing. To address these issues, enhancing their therapeutic potential, siRNAs can be modified controlling their role in the RNAi pathway. An *Ortho*-functionalized, tetrafluorinatedazobenzene was integrated into the siRNA backbone via phophoramidite chemistry to generate a class of photoswitchable F-siRNAs. These F-siRNAs retained the ability to photoisomerize from an active *trans* to an inactive *cis* state through blue and green light respectively. This thesis reported on a novel technique to inject single cell medaka embryos with both Wt and F-siRNAs. Medaka are a small freshwater teleost fish that have a number of desirable features for use as a vertebrate model in gene silencing projects. These attributes include daily spawning, a number of useful genetic strains, a completely sequenced genome, and a transparent egg.

Keywords: siRNA; Antisense; Japanese Medaka; Nano injection; Transgenic.

AUTHOR'S DECLARATION

I hereby declare that this thesis consists of original work of which I have authored. This is a true copy of the thesis, including any required final revisions, as accepted by my examiners.

I authorize the University of Ontario Institute of Technology (Ontario Tech University) to lend this thesis to other institutions or individuals for the purpose of scholarly research. I further authorize University of Ontario Institute of Technology (Ontario Tech University) to reproduce this thesis by photocopying or by other means, in total or in part, at the request of other institutions or individuals for the purpose of scholarly research. I understand that my thesis will be made electronically available to the public.

The research work in this thesis that was performed in compliance with the regulations of Research Ethics Board/Animal Care Committee under **REB Certificate number/Animal care certificate file number**.

Makenzie Mateus

YOUR NAME

STATEMENT OF CONTRIBUTIONS

I hereby certify that I am the sole author of this thesis and that no part of this thesis has been published or submitted for publication. I have used standard referencing practices to acknowledge ideas, research techniques, or other materials that belong to others. Furthermore, I hereby certify that I am the sole source of the creative works and/or inventive knowledge described in this thesis.

ACKNOWLEDGEMENTS

I would first like to acknowledge my supervisors Dr. Dennia Simmons and Dr Jean-Paul Desaulniers without both of you I would have never been able to complete this masters project. Thank you for always pushing me forward and to focus on the few successes over the many failures that come along with scientific research. This experience has not only allowed me to grow as a scientist but as a person as well. I have been lucky enough to have been in the Simmons lab for 4 years now and have loved every minute of helping out in the aquatic's facility. Through both of you I was able to travel and present our work, an experience I will never forget.

I would also like to extent my gratitude to Dr. Sean Forrester, for not only being involved in my thesis committee; but also, allowing me to use your lab to complete my experiments. Additionally, thank you for providing knowledge and support on this research which was invaluable.

My appreciation also goes out to my lab members in both lab groups. Matt without your training this project would not have been possible for that I am extremely grateful. To Virgina, Kevin, Ifrodet, and Autumn thank you for being the best lab mates possible. Truly, your guy's company made the long hours go by much quicker and I could not have asked for a better group to share this experience with.

To Theresa, I cannot express enough thanks and gratitude for all the things you have showed me.

Finally, I must recognize Jennifer Nichols without whom I would not have the strength to continue this project. I sincerely dedicate all my success to you, thank you.

TABLE OF CONTENTS

LIST OF FIGURES AND TABLES

CHAPTER 1

CHAPTER 2

CHAPTER 3

LIST OF ABBREVIATIONS AND SYMBOLS

Ago-2	Argonaute 2
BLT	Blue light treated
$CaCl_2$	Calcium Chloride
$CDCl_3$	Deuterated chloroform
CuCN	Copper Cyanide
DBU	1,8-Diazabicyclo[5.4.0]undec-7-ene
DCM	Dichloromethane
DMF	Dimethylformamide
DMSO	Dimethylsulfoxide
DMT	4,4'-Dimethoxytrityl
EDTA	Ethylenediaminetetraacetc acid
EMAM	Methylamine 40% in H_2O and Methylamine 33% in EtOH 1:1
eGFP	Enhanced green fluorescent protein
FDA	Food & Drug Agency
GalNAc	*N*-acetylgalactosamine
GLT	Green light treated
HAO1	Hydroxy acid oxidase 1
HCl	Hydrochloric acid
HOBt	Hydroxybenzotriazole
Hpf	Hours post fertilization
Hpi	Hours post injection
HPLC	High pressure liquid chromatography
KCl	Potassium Chloride
LDL-C	Low-density lipoprotein cholesterol
LC/MS	Liquid chromatography mass spectroscopy
$MgCl_2$	Magnesium Chloride
$MgSO_4$	Magnesium Sulfate
mRNA	Messenger RNA

NaCl	Sodium Chloride
$NaHCO_3$	Sodium bicarbonate
Na2HPO4	Disodium phosphate
NaOH	Sodium hydroxide
Na_2SO_4	Sodium Sulfate
NCS	N-Chlorosuccinimide
NH_3	Ammonia
NMR	Nuclear magnetic resonance
PCSK9	Proprotein convertase subtilisin/kexin type 9
RFU	Relative fluorescence units
RISC	RNA-induced silencing complex
RNAi	RNA interference
RNase	Ribonuclease
SCR	Scrambled sequence
siRNA	short interfering RNA
ssRNA	Single stranded RNA
TEAA	Triethylamine-Acetic Acid
Tg	Transgenic
TLC	Thin layer chromatography
THF	Tetrahydrofuran
TTR	Transthyretin
Wt	Wild type

Chapter 1: Introduction and Literature Review

1.1 Introduction

Gene silencing oligonucleotide molecules have become a popular therapeutic tool for treating genetic disorders over the past decade.[1] The short interfering RNA (siRNA) antisense molecule has emerged as one of these treatments due to its effective silencing of specific genes.[1] Currently, there are five siRNA therapeutic drugs on the market with more being FDA approved each year.[2] These five siRNA drugs predominantly target therapeutic areas including the nervous system, the cardiovascular system, endocrine functions, and metabolism. These areas encompass conditions such as amyloidosis, familial amyloid polyneuropathies, hyperlipidemia, and various other diseases. Although a useful therapeutic tool for genetic disorders, there are a variety of challenges to be overcome when using siRNAs which include toxicity, stability, tissue-specific targeting, off target effects, controlled-timing of activity, and prolonged silencing.[2,3,4] Much of the research conducted on the use of siRNAs for therapeutics is done on how they can be modified to overcome these setbacks.[4] This thesis reports on a tetrafluorinated azobenzene modified siRNA used to silence enhanced green fluorescent protein (eGFP) expressed in transgenic (Tg) Japanese medaka (*Oryzias Latipes*) potentially overcoming current antisense therapeutic challenges.

1.2 The RNAi pathway

The siRNA molecule is endogenous to human cells and acts to silence genes by cleaving messenger RNA (mRNA) during the RNA interference (RNAi) pathway.[3] The silencing mechanism begins when a long single stranded RNA (ssRNA) is synthesized in the nucleolus and forms a hairpin shaped structure due to each end being complementary

to each other.[3,4] The hairpin portion is cleaved by an endoribonuclease called Dicer. After cleavage, Dicer releases the siRNA strands which interacts with the protein Argonaute 2 (Ago-2), and others which form the RNA-induced-silencing-complex (RISC).[4] Once formed, the duplex is unwound, leaving the strand that is thermodynamically less stable due to its base pairing at the 5' end.[2,5] The single stranded siRNA, along with RISC, scan for complementary mRNA. Once found, the siRNA anneals to its target mRNA and Ago-2 cleaves the mRNA such that protein synthesis of that particular gene cannot occur.[4] Therefore, synthetic siRNA is utilized to target specific mRNAs transcribed from specific genes effectively acting as a gene silencer.[1] Pathway shown in figure 1

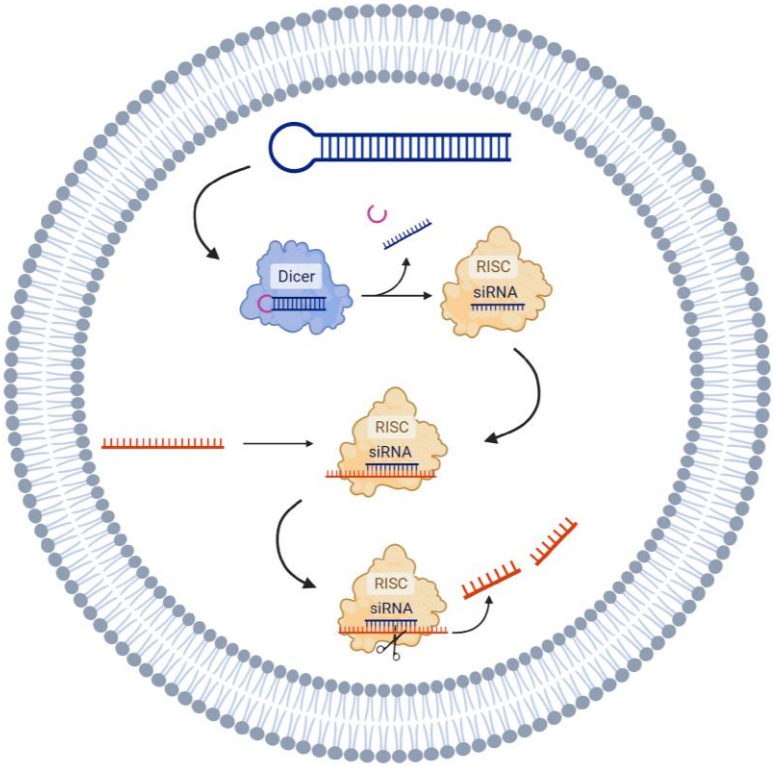

Figure 1.1 – Depicts the RNAi pathway. Long ssRNA forms a hairpin structure which is picked up by dicer and then digested into a single strand. A cascade of proteins including Ago-2 form the RISC complex and interact with the siRNA until a complimentary strand of mRNA is detected and bound to the entire complex. Once formed Ago-2 can cleave the mRNA specific to that siRNA which is then degraded in the cell preventing protein formation. Figure was made in Biorender.

1.3 The current use of siRNAs as therapeutics

The RNAi pathway prevents the translation of mRNA into protein due to the innate ability of siRNA to bind to and degrade complementary mRNA when in a complex with RISC. siRNAs act as gene expression suppressors and, depending on the mRNA targeted, this has great potential for therapeutic use. As a result, siRNAs have been intensely researched for the past few decades to design novel medications specific for gene-related diseases.

1.3.1 Patisiran (approved in 2018)

The first-ever FDA approved siRNA released to market was Patisiran in 2018 for the treatment of hereditary transthyretin-mediated amyloidosis.[3] In individuals with this condition, a mutated transport protein called transthyretin (TTR) accumulates in various organs and tissues, leading to organ damage and dysfunction.[3] Individuals with this rare disease suffer from a diverse array of symptoms ranging from organ damage and dysfunction to cardiomyopathy in more advanced cases.[6] Patisiran works by using siRNAs to target and silence the production of both mutated and wild type TTR protein encoding RNAs.[6] By reducing the levels of abnormal TTR, Patisiran slows the progression of the disease and can alleviate symptoms.[6] The approval of Patisiran marked a significant milestone in the field of RNAi therapy and opened the door for the development of other siRNA-based drugs for various diseases. Since then, four other siRNA drugs have been FDA approved – Givosiran, Lumasiran, Inclisiran, and Vutrirsan with more in development for other rare genetic disorders.

1.3.2 Givosiran (approved in 2019)

Like Patisiran, Givosiran exerts its mechanism of action through RNAi silencing.[3] It mediates its effect by targeting the aminolevulinate synthase 1 mRNA, found in the liver, which leads to the decrease of aminolevulinic acid (ALA) in the blood stream. When irregular amounts of ALA build up this leads to the disease acute hepatic porphyria.[6] To ensure the siRNA agent is taken up by hepatocytes the strand is conjugated with a trimer *N*-acetylgalactosamine (GalNAc) ligand.[6,7] This uptake into the liver occurs due to the GalNAc trimer binding to the Asialoglycoprotein receptor (ASGPR) that is predominantly expressed on liver hepatocytes.[7] Upon binding the siRNA ligand conjugate is engulfed into the hepatocyte through endocytosis; then, due to a drop in pH the siRNA is unbound to both GalNAc and the ASGPR.[7] Through a currently unknown mechanism a small portion of siRNA can make its way out of the endosomal bilayer and participate in RNAi in the cytoplasm of the hepatocyte.[7]

1.3.3 Lumasiran (approved in 2020)

Lumasiran works through RNAi in the liver resulting in cleavage and breakdown of its target, hydroxy acid oxidase 1 (HAO1) mRNA.[6] Through a series of pathways, HAO1 leads to the production of a mutated version of the enzyme alanine glyoxylate aminotransferase in patients with primary hyperoxaluria type 1.[6] To ensure siRNA absorption into liver hepatocytes, a GalNAc modification is used on the Lumasiran siRNA, thus permitting drug efficacy.[6]

1.3.4 Inclisiran (approved in 2021)

Inclisiran produces effects through RNAi in liver hepatocytes by silencing the expression of proprotein convertase subtilisin/kexin type 9 (PCSK9), an enzyme which

degrades hepatic low-density lipoprotein cholesterol (LDL-C) receptors.[6] The siRNA sense strand is bound to the GalNAc ligand which allows hepatocytes to uptake the siRNA and target PCSK9.[6,7] This action promotes the expression of LDL-C receptors on the cell surface and facilitates receptor cycling.[6] Lysosomal enzymes can degrade LDL-C once bound to its receptor resulting in re-uptake into cells reducing its levels in the blood.[6] High levels of LCL-C in their bloodstream can be toxic and can lead to heterozygous familial hypercholesterolemia or clinical atherosclerotic cardiovascular disease which causes atherosclerosis in the arteries over time.[6]

1.3.5 Vutrisiran (approved in 2022)

Vutrisiran works as a double stranded siRNA which targets transthyretin mRNA, a protein created in the liver that transports vitamin A.[8] Mutations in this gene result in patients with transthyretin amyloidosis, a disease caused by large deposits of misfolded transthyretin called amyloids located in the heart and peripheral nerves.[8,9] Again, Vutrisiran works in the liver, so GalNAc is ligated to the siRNA which increases uptake into hepatocytes, where the siRNA reduces levels of transthyretin mRNA, both mutated and wild type, consequently reducing the expression of amyloid deposits.[8,9]

1.4 The current challenges siRNAs face for drug development

Each siRNA drug currently on the market or currently in development has a specific chemical modification to overcome the innate challenges they face for use as therapeutics. Although they are a useful tool to silence mutated genes that cause genetic diseases, siRNAs have issues with toxicity, stability, tissue-specific targeting, off target effects, and controlled-timing of activity.[2,3,4] With respect to toxicity, siRNAs are generally well tolerated; however, in some cases they can cause an innate immune response. Previous

work demonstrating siRNAs that are approximately 23 nucleotides in length trigger an interferon response causing cell death.[10] Additionally, if the sequence has a high GU content, then it could bind to and over activate toll-like receptor 7, which has been associated with diseases such as lupus.[10] Thus, it is important to design sequences that minimize any negative effects on their intended tissue and host by further researching the mechanism in which an interferon response occurs and limiting the GU nucleotide content of sequences.

To be effective as therapeutics, siRNAs must endure throughout the body without being degraded or metabolized by an endogenous enzyme. This is a challenge due to extracellular siRNAs being highly susceptible to ribonucleases (RNases) which play an important role in almost every aspect of RNA metabolism including maturation, degradation, turnover, and quality control.[11] Moreover, additional challenges that effect stability are due to the half-life of naked siRNAs being measured from minutes to days in serum.[12,13] Even if longer-lived, targeting of specific tissues remains an issue. This stems from the large size and overall negative charge of siRNA, which prevents them from diffusing across cellular membranes.[10] When looking at current siRNA drugs, GalNAc is used to specifically target hepatocytes; however, not every tissue-type has such an elegant solution at the moment. Even when GalNAc is used to enter the cell, escape from the endosome must also be considered as very little of an siRNA <1% is actually released into the cytoplasm via endocytosis.[7] Finally, once in the cytoplasm, the siRNA remains vulnerable to cellular RNases – and any modifications to prevent siRNA degradation must still allow for RISC to recognize it and perform RNAi.

Even when identified properly by RISC, the RNAi pathway can cause more harm than good through involuntary off-target effects. This is due to the suppression of important genes other than the intended target. Studies have shown that off target-effects can occur when an siRNA has partial (6 to 7 base pairs) nucleotide homology with an unintended mRNA transcript leading to the suppression of the similar gene.[14,10] When this occurs, undesirable mutations in gene expression can lead to dangerous side effects such as cell death or exacerbated cell transformation.[10] This may be caused by a similar oligonucleotide gene suppression phenomenon called microRNA in which siRNAs behave as them.[15] Moreover, selection of the sense strand instead of the desired antisense strand by RISC can lead to consequential degradation of unintended mRNA.[10] It is only through in vivo testing and precise modification of siRNA sequences that off-target silencing can be eliminated from the gene suppression mechanism.

Finally, although stability of siRNAs is an issue controlling the timing of activation is important as well as due to prolonged silencing. Each of the FDA approved siRNA therapeutics are long lasting which in most cases is useful for us as medication; however, there could be some instances where you may not want an siRNA to exert its effects for this prolonged period. Therefore, there is a need to inactivate the activity of an siRNA. This is highlighted in Zlatev *et al* 2018 wherein they found that GalNAc ligated siRNAs when administered caused hepatoxic effects in mice.[16] With the addition of their novel technology REVERSIR they were able to attenuate these hepatoxic findings.

1.5 Chemical modifications made to siRNAs to increase therapeutic potential

Chemical modifications can be made to overcome the current challenges siRNAs face as therapeutics. Different modifications have been shown to increase stability and

cellular uptake (such as GalNAc) to specific tissues.[7,17] Every part of the siRNA molecule has been thoroughly investigated from its sugar residues, backbone, and nucleotide bases. Each with the objective to engineer an siRNA that is not held back by negative limitations.

Currently, some of the most promising modifications come from changes to the sugar and phosphate backbone moiety. Present alterations include changing the 2′-H to a 2′-Fluro, 2′-O-methyl, or 2′-O-methoxyethyl, all of which increase the stability of the molecule in serum due to adopting an energetically favourable confirmation.[17,10] Furthermore, it was demonstrated guanine and uracil residues that were modified with a 2′-O-Me had reduced immunostimulation and interferon response.[17,18] However, to increase resistance against nucleases, further improving stability, backbone modifications can be used. For example, to make siRNAs more stable, modifications with phosphothioate, boranophosphate, and phosphorodithioate have been developed.[10,17] With respect to the phosphothioate modification, stability was improved in nuclease dense solution, while cellular uptake and silencing ability remained constant; but was toxic to HeLa cells.[19] This prompted a change to boranophosphate which increased nuclease resistance by 10-fold while not causing any cytotoxic effects nor reducing silencing ability.[17,20] In more recent years phosphorodithioate modifications have been used in which target gene expression has been minimized and serum stability increased.[17]

Finally, siRNA nucleobase modifications have been explored with a high degree of success. Substituting a 5-fluoro-2′-deoxyuridine throughout multiple locations on an siRNA molecule enhanced cytotoxicity levels *in vitro* by more than 10-fold, with in some cases a 100-fold increase in toxicity.[21] It was reported that the thermodynamic stability was higher in siRNAs modified with a lipophilic boron cluster, 3-*N*-[(1,12-dicarba-closo-

dodecacarboran-1-yl)propan-3-yl]thymidine at N3 position of the sense and anti-sense strand which in turn raised the stability of the molecule.[22] Overall, the modifications mentioned above are just a handful of the current set with more being researched all the time. One thing that is clear is that the type of modification, along with the motif that is being modified, dictates how the siRNA is changed (not one or the other individually) whether it be increased gene silencing, increased stability, reduced cytotoxicity, or which tissue is targeted.

Currently, many of the modifications made to the siRNA structural motif have resulted in oligonucleotides with increased silencing and stability while reducing cytotoxicity. GalNAc ligated siRNAs prove effective in hepatocyte-specific targeting. Research needs to be done to target other tissues, to solve the problem of off-target effects, and more importantly, controlled timing and activity of an already deployed siRNA once in the cell. One solution to this latter problem is to modify siRNAs with azobenzene: a photoswitchable molecule used in biological processes to enhance modulation, effectively turning the molecule on or off.

1.6 Azobenzene

Azobenzene has the ability to absorb and reflect UV light; due to this, azobenzene has been used to make dyes in the past. However, the Desaulniers lab's interest in azobenzene is because of its ability to photo isomerize, which was first detected in 1937 by G.S Hartley.[23] The structure includes a nitrile bond that connects two benzene molecules (**Figure 1.2**) and it is this unique structure that allows an azobenzene molecule to switch conformation from *trans* to *cis* state when exposed to UV light.[24] Similarly – after this

conformational change by UV light – when exposed to visible light the molecule can relax, reverting back to its *trans* state.[25]

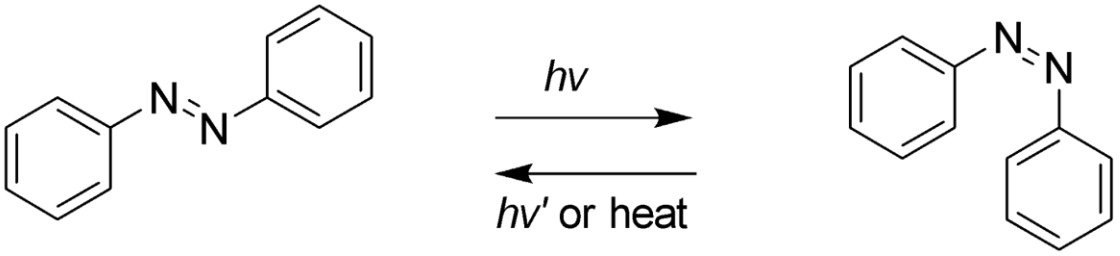

Figure 1.2 - Conformational change of azobenzene from *trans* (right) to *cis* (left) state when exposed to UV light and the reverse change when exposed to visible light or heat energy.

1.6.1 Tetrachlorinated azobenzene

Research into azobenzene has rapidly evolved over the past several years due to its incorporation into biological systems as a rapid and dependable method of modulation. However, the dependence of this system on UV light, causes problems in biological systems, because UV light has poor tissue penetration, can damage DNA, and damage DNA repair mechanisms; thus, there can be toxic side-effects.[26] To overcome UV toxicity, chemical modifications have been implemented to azobenzene molecules so that UV light is no longer needed for a conformational change. Past iterations of this include the insertion of four chlorine atoms at the *ortho* positions along the azobenzene molecule.[27] When exposed to red light, chlorinated azobenzene molecules will red-shift, transitioning from *trans* to *cis* state.[27] Irradiation with violet light allows the molecule to relax back to *trans* state.[27] Additionally, when chlorinated azobenzene is incorporated into the backbone of an siRNA molecule, it retains the ability to photo isomerize.[27] However, since siRNAs are used for therapeutic purposes, the addition of chlorine may not be an ideal chemical modification. The chlorine atoms near the nitrogen linker can destabilize the molecule due

to the bulkiness of the atom. Moreover, chlorinated benzenes are notoriously toxic (e.g., dioxins, furans, and PCBs).[28] Therefore, a substitution that increases molecular stability, is safe in biological systems, and decreases the energy requirement for azobenzene excitation should be used.

1.6.2 Tetrafluorinated azobenzene

When compared to chlorine, fluorinated azobenzene should have a larger red-shift, meaning more wavelengths of visible light could be used to perform the conformational switch.[26,27] Both chlorine and fluorine act as electron withdrawing groups through the inductive effect weakening the pi bonded nitrogen's; however, fluorine is smaller than chlorine making the final structure more stable.[29] Previously it has been reported that the half-life of fluorinated *cis*-azobenzene is about 15 minutes at 95 °C which is substantially longer when compared to chlorinated *cis*-azobenzene's half-life, of about 1 minute.[27,29] Finally, the conformational change from *trans* to *cis* state can be controlled with longer wavelengths of visible light when compared to chlorinated azobenzene reducing the risk of cell damage.[27,29] To that end, when inserted into oligonucleotides fluorinated azobenzene siRNAs (F-siRNAs) should overcome the off-target effects since it can be easily switched on, with blue light, and off, with green light, therefore better regulating the gene silencing process depicted in **Figure 1.3**.

1.6.3 Tetrafluorinated azobenzene functionalized siRNA

As stated above, the Desaulniers lab has had previous success using o*rtho*-functionalized tetrafluorinated azobenzene siRNAs to silence firefly luciferase mRNA in HeLa cells.[29] Due to the photoswitchable nature of fluorinated azobenzene the thought was that when in the *cis* confirmation, which can be initiated through green light exposure, the

siRNA double helix would be distorted preventing RISC loading deactivating gene silencing. Thus, when exposed to nontoxic green light at 530nm wavelength, any gene silencing would stop in transfected cells; however, if exposed to blue light at 470nm wavelength, gene silencing could be reactivated. Controlling the activation of gene expression through minimal non-toxic light exposure would make F-siRNAs a beneficial therapeutic tool being of use in clinical settings. The F-siRNAs were transfected in HeLa cells at different concentrations and results showed after exposure to a blue light treatment for 1 hour post transfection there was significant knockdown from control levels when measured at 24 hours post transfection using a luciferase assay.[29] Blue light treated HeLa cells were assayed again at 48 hours and 72 hours post transfection, during the latter time point 80% knockdown was achieved.[29] The green light treated cells showed control levels of luciferase expression at all time points suggesting an inactive siRNA state. Additional tests exposed the cells to green light for 1 hour post transfection then after a rest period the cells were exposed to blue light for 1 hour, suggesting the azobenzene molecular switch can go from a *cis* to *trans* state as the results indicated through luciferase knockdown.[29]

To further demonstrate the ability of the molecular switch inactivating and reactivating the siRNA, a variation of green to blue to green light exposure tests were completed. These included a test where at time point 0 hours and 24 hours post transfection green light was used, with a blue light treatment in between at time point 2 hours.[29] At 48 hours and 72 hours luciferase activity was measured at near control levels of activity.[29] This suggests the fluorinated azobenzene switch can flip from *cis* to *trans* and then back to *cis* states. One final test with an added blue light exposure at time point 26 hours post transfection was run showing slightly lower knockdown than in the previous experiments

but still significantly different.[29] Again, this suggests the switch can flip from *cis* to *trans* back to *cis* back to *trans* reactivating and deactivating the gene silencing mechanism through a simple light treatment.

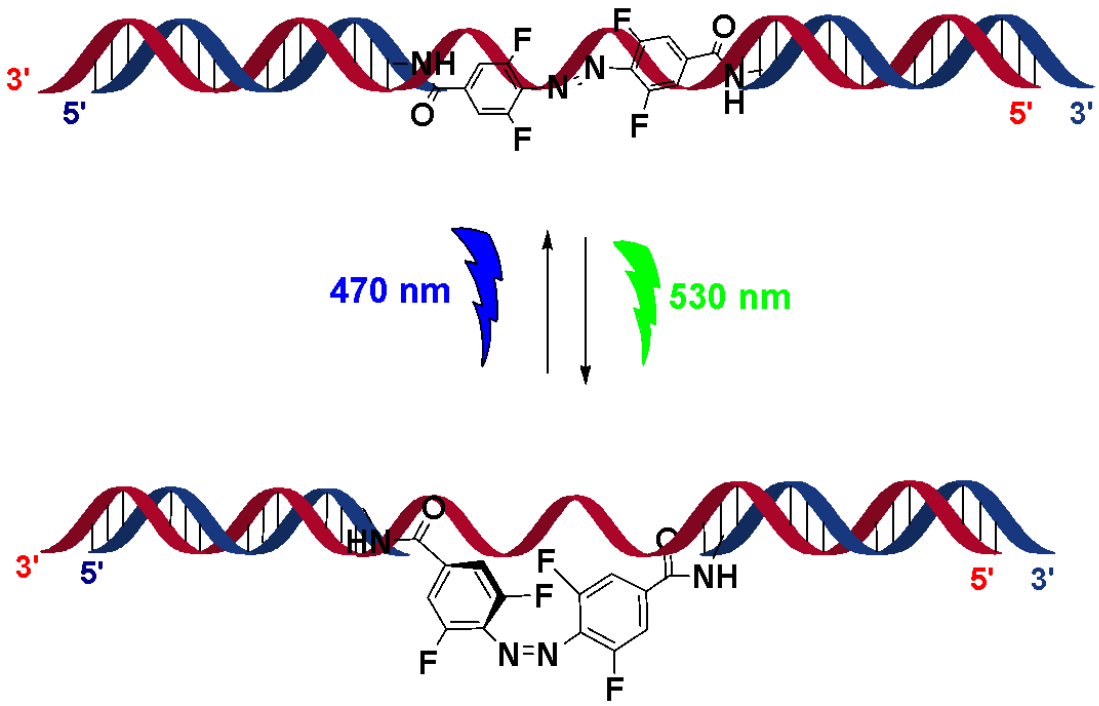

Figure 1.3 - Shows the conformational change mechanism of fluorinated azobenzene inserted into the backbone of an siRNA from trans (active) to cis (inactive) state using green light at 530nm and then back using blue light at 470nm.

1.6.4 How F-siRNAs could work as a therapeutic drug

From the current data collected of F-siRNAs in HeLa cells, it is clear that these antisense therapeutics could work with a photoswitch. In theory, off-target effects could be availed by treated the target tissue/area with green light, inactivating the gene silencing activity of the F-siRNA thus mitigating any off-target effects. However, most internal areas of the body can not be exposed to visible light exposure without invasive probing. To that end, the current idea to fully utilize the therapeutic potential of F-siRNA would be to target ocular diseases. Unlike skin, the eye allows for visible light to pass through to deeper layers

of the tissue making it a functional candidate to target, much like how GalNAc ligated siRNAs are specific to mRNA synthesized in the liver. Furthermore, the idea of using siRNAs for the treatment of eye disorders is not unheard of. Glaucoma is one of the leading causes of permanent blindness around the world caused by an increase in intraocular pressure that can be due to a variety of different neuropathies.[30] Sometimes this pressure results from a build-up of misfolded mutant proteins in the eye, other times it can be due to Na-K-ATPase misfunctioning.[30,31] As such, there have been a variety of attempts to use siRNA therapeutics to alleviate the symptoms of the condition. In fact, there are other ocular diseases in which siRNAs could be a viable solution. Diseases that have been researched in the past include wet age-related macular degeneration, diabetic retinopathy, retinitis pigmentosa, corneal neovascularization, fibrotic eye diseases, and various inherited retinal diseases.[30,31] Overall, this previous ocular research would serve as a blueprint for what could be a promising new approach to siRNA therapeutics in which gene expression could be turned on and off through a simple treatment of visible light.

1.7 Japanese medaka as a *in vivo* model

Before any drugs can be FDA approved for public use they must first go through extensive testing. One of the preliminary stages of siRNA drug development is *in-vivo* testing for proof of concept.[32] Useful species for projects such as these includes the use of a fish embryo system. Japanese medaka (*Oryzias Latipes*) are a small freshwater teleost fish that have desirable features for use as a vertebrate model.[33] These attributes include daily spawning, availability of a number of useful genetic strains, a completely sequenced genome, and a transparent egg chorion - the latter two of which might be the most important for this study.[33,34] Transparency allows for the precise introduction of DNA, RNA, or

protein solutions directly into the cytoplasm of the egg through microinjection.[34] Additionally, visible light should easily penetrate the membrane, thus enabling photo-switchable control of gene expression while also being able to observe development of the embryo. Furthermore, knowing the entire genome allows us to create siRNAs with greater confidence that they will bind to their target mRNA. Due to daily spawning, multiple experiments can be run throughout the week allowing for a plethora of data collection while having several useful genetically modified medaka strains allows us to pick traits that are specific to our research goals.

The Japanese medaka strain used in this study were obtained from the National BioResource Project [NBRP] in Japan and are a transgenic (Tg) medaka strain denoted as d-rR-Tg(beta-actin-loxP-GFP). In this strain, expression of enhanced green fluorescent protein (eGFP) occurs throughout the whole body after midblastula transition. We chose this strain so that we could target the eGFP gene, as there should be no toxic effect to the overall organism when the gene is silenced, and we can measure the amount of silencing by reduction in fluorescence using a plate reader.

1.8 eGFP as a gene target

The current idea is that synthetic siRNAs targeting eGFP can be injected into the Japanese medaka embryo, then during a later time eGFP expression will be measured and compared to a selection of controls. Not only has GFP been used in similar silencing studies before, but it has been used in fish, specifically rainbow trout.[35] This research group was able to show using a range of siRNAs at different concentrations, the suppression of GFP in Tg rainbow trout was significant after microinjection into the embryo.[35] Due to the similarities between rainbow trout and Japanese medaka, the same principles of siRNA

technology should apply allowing us to show consistent knockdown in Tg medaka.[35] In fact, medaka have been the focal point of siRNA research before when a group used both siRNAs and morpholinos to supress the YPEL gene, responsible for cellular proliferation and growth.[36] One final note of concern, like all proteins, eGFP has a half-life, in this case is approximately 26 hours.[37] This should be considered when measuring the final amounts of eGFP within each Tg embryo after siRNA are injected.

1.9 Rational and objectives

The overall objective of this research project was to photocontrol expression of gene targets in Japanese medaka. To achieve this goal, we chemically synthesized the fluorinated azobenzene molecule and inserted this into an siRNA molecule that is designed to be complementary to gene targets within Japanese Medaka. Then we injected these tetrafluorinated azobenzene-containing siRNAs into one-cell stage embryos and tested the ability of visible light to penetrate and control the photo-switch *in-vivo*. If the eGFP gene we have selected is silenced, this will demonstrate the first proof-of-concept in an *in-vivo* vertebrate system. The research conducted throughout this project will develop a novel siRNA gene silencing system in Japanese medaka with the intention to flip the molecular switch on the F-siRNAs developed by the Desaulniers group. These are an innovative approach to solving current problems RNA gene silencing technology faces today such as, controlling the timing in which gene silencing happens and by extension, controlling off-target effects. Additionally, this project can answer questions surrounding the functionality of these F-siRNAs such as:

1) Will the photoactive light switch work in our Japanese medaka embryos?
2) How long will our siRNAs remain active?
3) Are the siRNAs capable to flip from *trans* to *cis* state and vice versa?
4) Is the RISC complex functional within early embryos?

Overall, this is all for the development of potentially life enhancing medical technologies and thus can greatly impact all our lives. This project can be broken down into two research phases:

1. Chemical synthesis of F-siRNAzo's:
    a. Synthesizing the fluorinated azobenzene molecule.
    b. Designing/finding an antisense molecule strand that silences the eGFP.
    c. Incorporating the fluorinated azobenzene into the backbone of the antisense siRNAs using phosphoramidite chemistry.
2. Testing *in-vivo*, injecting the antisense molecules into one-cell stage embryos:
    a. Medaka culturing and breeding to obtain one-cell stage embryos.
    b. Injection of the wt and F-siRNAs into one-cell stage embryos.
    c. Demonstrate if the molecular azobenzene switch works *in vivo* – detecting fluorescence changes in the embryos.
    d. Injection of the scrambled wt and scrambled F-siRNAs into one-cell stage embryos.

Chapter 2: Methods

2.1 F-Azobenzene Synthesis

All starting materials and solvents used throughout the chemical synthesis of this master's thesis were obtained from either Sigma-Aldrich or TCI, unless otherwise indicated. To dry down liquids to a concentrated form a rotary evaporator or a Gene Vac miVac Quattro concentrator were used. Products were purified manually using flash column chromatography with Silicycle Siliaflash P60 (230-400 mesh). A Bruker Ascend 400MHz NMR spectrophotometer was used to obtain ^{1}H NMRs recorded for 64 transients at 400MHz ^{31}P NMRs. To process and integrate spectra ACD labs NMR processor Academic Edition was used. Synthesis of compound 9 was completed by Matthew Hammill and the overall chemical schematic was designed by Kota Tsubaki

2.1.1 Synthesis of 4-bromo-2,6-difluoroaniline: Compound (2)

To a round bottom flask containing 2,6-difluoroaniline (Compound 1) (12.9 g) in 200 ml of acetonitrile was added NBS (17.8 g) This mixture was stirred at room temperature for 24 hours and then concentrated under reduced pressure. The resulting crude product was then extracted using water and hexanes, and the organic solution was dried over Na_2SO_4. This solution was concentrated to purify the crude residue column chromatography was used (Dichloromethane (DCM) / Hexanes = 1 / 1) resulting in 2,6-difluoro-4-bromoaniline (compound 2) as a purple crystal powder. (19.03 g, 91%), ^{1}H NMR (400 MHz, $CDCl_3$) δ 7.01 (dd, $^{3}J_{H,F}$ = 5.2 Hz, J = 1.2 Hz, 2H), 3.59 (br, 2H).

2.1.2 Synthesis of 4-amino-3,5-difluorobenzonitrile: Compound (3)

To a round bottom flask containing compound 2 (1.78 g) in DMF (15ml), CuCN (2.3 g) was added. This mixture was refluxed at 150 °C for 24 hours and then filtrated under

pressure using a 12% aqueous solution of NH_3 . The resulting filtrate was then washed using water and ethyl acetate and the organic solution was dried over Na_2SO_4. During this step an emulsion would form, to fully separate the two layers NaCl solution in excess was used as the water layer. To purify the crude residue column chromatography was used (DCM / Hexanes = 1 / 1) resulting in 4-amino-3,5-difluorobenzonitrile (compound 3) as a white solid (998 mg, 75 %). ^{1}H NMR (400 MHz, $CDCl_3$) δ 7.16 (dd, $^3J_{H,F}$ = 4.0 Hz, *J* = 2.0 Hz, 2H), 4.29 (br, 2H)

2.1.3 Synthesis of 4-amino-3,5-difluorobenzoic acid: Compound (4)

To a round bottom flask containing compound 3 (1.78 g), a 1M NaOH aqueous solution was added. This mixture was refluxed for 16 hours and then was quenched dropwise until (pH =1) salts participated by the addition of a 1M solution of HCL. The crude solution was then filtered with the remaining participate being dissolved in ethyl acetate. The resulting filtrate was then extracted using water and ethyl acetate, and the organic solution was dried over Na_2SO_4 and concentrated under reduced pressure resulting in 4-amino-3,5-difluorobenzoic acid (compound 4) as an orange solid (932 mg, 99 %). ^{1}H NMR (400 MHz, DMSO-d_6) δ 12.68 (br, 1H), 7.39 (dd, $^3J_{H,F}$ = 7.2 Hz, *J* = 2.36 Hz, 2H), 3.35 (br, 3H)

2.1.4 Synthesis of 4-amino-N-(2-((tert-butyldimethylsilyl)oxy)ethyl)-3,5-difluorobenzamide: Compound (5)

A round bottom flask containing compound 4 (1.11 g), 2-((*tert*-butyldimethylsilyl)oxy) ethanolamine (1.12 g), HOBT (81 mg) and EDC・HCl (1.22 g) was stirred at room temperature for 24 hours in 12 ml of DMF. The mixture was then extracted using water and ethyl acetate and dried over Na_2SO_4. To purify the crude residue column chromatography was used (Ethyl acetate / Hexanes = 1 / 2) resulting in 4-amino-

N-(2-((tert-butyldimethylsilyl)oxy)ethyl)-3,5-difluorobenzamide (compound 5) as a white solid. (1.65 g, 85 %), ^{1}H NMR (400 MHz, $CDCl_3$) δ 7.29 (d, $^{3}J_{H,F}$ = 2.0 Hz, 2H), 6.41 (br, 1H), 3.79 (t, *J* = 5.6 Hz, 2H), 3.55 (q, *J* = 5.2 Hz, 2H), 0.93 (s, 9H), 0.097 (s, 6H).

2.1.5 Synthesis of (E)-4,4'-(diazene-1,2-diyl)bis(N-(2-((tert-butyldimethylsilyl)oxy)ethyl)-3,5- difluorobenzamide: Compound (6)

A round bottom flask containing compound 5 (0.12 g) in 5 ml of DCM had DBU (0.11g, 7.2 mmol) and NCS (0.95g, 7.2 mmol) added after being placed in a dry ice bath at -78 ℃. The reaction solution was stirred for 20 minutes before having 15 ml of $NaHCO_3$ added and then washed with water three times to extract any impurities. To purify the crude solution column chromatography was used (Ethyl acetate / Hexanes = 1 / 2) resulting in E)-4,4'-(diazene-1,2-diyl)bis(N-(2-((*tert*-butyldimethylsilyl)oxy)ethyl)-3,5-difluorobenzamide (compound 6) as an orange solid. (0.20g, 84%), ^{1}H NMR (400 MHz, $CDCl_3$) δ 7.48 (d, $^{3}J_{H,F}$ = 9.2 Hz, 4H), 6.57 (t, *J* = 5.2 Hz, 2H), 3.83 (t, *J* = 4.8 Hz, 4H), 3.61 (q, *J* = 5.2 Hz, 4H), 0.94 (s, 18H), 0.12 (s, 12H).

2.1.6 Synthesis of (E)-4,4'-(diazene-1,2-diyl)bis(3,5-difluoro-N-(2-hydroxyethyl)benzamide): Compound (7)

A round bottom flask containing compound 6 (1.21 g) in 10 ml of ethanol had 10 ml of 1% HCL in ethanol added. The reaction was stirred under argon for 3 hours and then concentrated under reduced pressure. After the molecule was washed with methanol and an extraction using water and hexanes was done before being concentrated under reduced pressure resulting in E)-4,4'-(diazene-1,2-diyl)bis(3,5-difluoro-N-(2-hydroxyethyl)benzamide) (compound 7) as a reddish brown solid (0.73 g**,** 90%). No further purification method was conducted on the product as it would not dissolve in a usable

solvent for flash column chromatography and NMR showed minimal impurities. ^{1}H NMR (400 MHz, DMSO-d_6) 8.82 (t, J = 5.44 Hz, 2H), 7.84 (d, $^{3}J_{H,F}$ = 10.16 Hz, 4H), 3.54 (t, J = 6.2 Hz, 3H), 3.36 (q, J = 5.72 Hz, 2H), 3.17 (s, 2H)

2.1.7 Synthesis of (E)-N-(2-(bis(4-methoxyphenyl)(phenyl)methoxy)ethyl)-4-((2,6-difluoro-4-((2-hydroxyethyl)carbamoyl)phenyl)diazenyl)-3,5 difluorobenzamide: Compound (8)

To a round bottom flask containing anhydrous pyridine (5 ml), compound 7 (0.20 g) was added. After the compound was fully dissolved, 4,4'-dimethoxytrityl chloride (DMT) (0.158 g) was added, and the solution was stirred for 24 hours under argon. The mixture was monitored by TLC (Methanol : DCM = 1/20) and then concentrated under reduced pressure before being purified by flash column chromatography (Methanol 5% to 10% in DCM), which resulted in a dark red oil (0.341 g, 60%). ^{1}H NMR (500 MHz, CDCl3) (E isomer) δ 7.28-7.17 (m, 13H), 6.88 ((t, J = 5.3 Hz, 1H), 6.84-6.81 (m, 4H), 6.47 (t, J = 5.4 Hz, 1H), 3.87-3.84 (m, 2H), 3.77 (s, 6H), 3.66-3.61 (m, 4H), 3.41 (t, J = 5.0 Hz, 2H).

2.1.8 Synthesis of (E)-2-(4-((4-((2-(bis(4-methoxyphenyl)(phenyl) methoxy)ethyl)carbamoyl)-2,6-difluorophenyl)diazenyl)-3,5difluorobenzamido)ethyl (2-cyanoethyl) diisopropylphosphoramidite: Compound (9)

To a flame dried round bottom flask, compound 8 (0.22g), THF (5 ml), anhydrous triethylamine (0.420 ml), and 2-cyanoethyl N,N-diisopropylchlorophosphoramidite (0.45 ml) were added. The reaction mixture was stirred at room temperature and monitored using TLC until starting material was used up around 3 hours. After concentrating the mixture by reduced pressure, the compound was purified on a silica gel column (Acetone / Ethyl acetate / Triethylamine = 86%: 10%: 4%) resulting in compound 9 as a dark red oil (0.15

g, 60%). ^{1}H NMR (400 MHz, CDCl3) δ ppm 7.44- 7.30 (m, 13H), 7.18 (d, *J* =9.05 Hz, 2H), 6.78 - 6.87 (m, 4H), 3.78 - 3.80 (m, 6H), 3.66-3.61 (m, 4H),2.16 - 2.20 (m, 4H), 1.17 - 1.24 (m, 12H). 19F NMR (377 MHz, (CD3)2CO) δ ppm -120.3 (s), -121.0 (s), -121.1 (s).

2.2 RNA synthesis and purification

The standard β-cyanoethyl 2'-*O*-TBDMS protected phosphoramidites, reagents and solid supports used to synthesize the Wt and F-azobenzene modified antisense strands were purchased from ChemGenes corporation and Glen Research. The complimentary sense strands were purchased from Integrated DNA Technologies. Strands were synthesized with a sequence intended to target the eGFP gene shown in **Table 1.**[38] Standard phosphoramidites were dissolved to a concentration of 0.10 M in anhydrous acetonitrile while synthesized azobenzene amidites were dissolved in a mixture (anhydrous acetonitrile / THF = 75%:25%) to a concentration of 0.10 M. Phosphoramidite coupling cycle reagents include acetic anhydride/pyridine/THF (Cap A), 16% N-methylimidazole in THF (Cap B), 0.25 M 5-ethylthio tetrazole in ACN (activator), 0.02 M iodine/pyridine/H_2O/THF (oxidation solution), and 3% trichloroacetic acid/dichloromethane. Each sequence was synthesized on a 1.00 μM dT solid support column running for a coupling time of 999 seconds using an Applied Biosystems 394 DNA/RNA synthesizer operating at a 1.00 μM cycle kept under argon at 55 psi. Each cycle consists of five steps: an acid catalyzed deprotection of DMT in which a primary alcohol reacts with the 2' phosphoramidite of the next base in the sequence. An activation step where diisopropylamine is displaced from the phosphoramidite by reacting with ethylthiotetrazole. A coupling step due to the exposed primary alcohol attacking the phosphoramidite linking the bases together. An oxidation step where phosphite is converted to phosphate through water, pyridine, and iodine. The

cycle will then either continue coupling the next base or when fully synthesized oligonucleotides can be cleaved from the solid support. Once each cycle was completed the columns were detached off the synthesizer and stored at 4 °C after being placed in a sealed tube. Using 1 ml of EMAM (methylamine 40% in H_2O / methylamine 33% in ethanol = 1:1 (Sigma-Aldrich)) oligonucleotides were cleaved from their respective columns leaving the solution in contact with the pore glass for 1 hour. To fully deprotect the bases the columns were left to incubate in EMAM solution overnight. The next morning the samples were concentrated under reduced pressure and resuspended carefully in DMSO:3HF/TEA (100 µL:125 µL). To remove the 2'-*O*-TDBMS protecting groups the solution was incubated at 65 °C for 3 hours. To desalt the RNA, the strands were placed in dry ice for 1 hour after being precipitated in ethanol and centrifuged at 4 °C for 30 minutes. Oligonucleotides were then run through Millipore Amicon Ultra 3000 MW cellulose. Equal concentrations of sense and antisense RNA were annealed by heating complimentary strands to 95 °C for 2 minutes in binding buffer (75.0 mM KCl, 50.0 mM TrisHCl, 3.00 mM $MgCl_2$, pH 8.30) and allowing the solution to cool to room temperature.

Strand	siRNA sequence	Target
Wt-siRNA-G1	3’-dtdt GUU CGA CUG GGA CUU CAA G-5’(s) 5’-CAA GCU GAC CCU GAA GUU Cdtdt -3’ (as)	eGFP
F-siRNA-G1	3’-dtdt GUU CGA CUG GGA CUU CAA G-5’(s) 5’-CAA GCU GAC AzoU GAA GUU Cdtdt -3’(as)	eGFP
SCR-F-siRNA-G2	3’-dtdt GUA CGU CGU GAG CUU ACA G-5’(s) 5’-CAU GCA GCA AzoC GAA UGU Cdtdt -3’ (as)	N/A

Tabel 2.1 Oligonucleotide strands that were tested on transgenic Japanese Medaka embryos expressing eGFP. WT-siRNA-G1 reflects the full unmodified sequence used to silence eGFP while F-siRNA-G1 represents the tetrafluorinated azobenzene modified siRNA. SCR denotation represents a scrambled sequence used to act as a control. *Incorporation of the azobenzene modification denoted as Azo at site in strand.

2.3 LC/MS characterization

LC/MS chromatograms were obtained on an Agilent 6545 QTOF-MS with Agilent 1260 Infinity Binary Pump HPLC using a ZORBAX Eclipse Plus C18 2.1x100mm 1.8-Micron Agilent column and a mobile phase of 5 mM ammonium acetate buffer (pH 7)/acetonitrile (95:5). Sample preparation included diluting oligonucleotides to a concentration of 0.01 O. D/μL. An injection volume of 20 μL/ sample was used. Data was analyzed using MassHunter Workstation Qualitative Analysis Software (Qual. 10.0).

2.4 HPLC characterization

Using a Waters 1525 binary HPLC pump with a waters 2489 UV/Vis detector and C18 4.6 mm x 150 mm reverse phase column, HPLC chromatograms were taken. Empower 3 software was for analysis of scans. An injection volume of 100 μL/ sample was used while running the column at 5% acetonitrile in 95% 0.1 M TEAA (Triethylamine-Acetic Acid) buffer up to 100% acetonitrile over 30 min.

2.5 Duplex characterization – Circular Dichroism experiments

CD spectra were calculated by averaging three replicates on Jasco's Spectra Manager version 2 software, ran on a Jasco J-815 CD equipped with a temperature controller. Equal concentrations of sense and antisense strands were annealed in 999 μL of CD sodium phosphate buffer (90.0 mM NaCl, 10.0 mM Na_2HPO_4, 1.00 mM EDTA, pH 7.00) by heating complimentary strands to 95 °C for 2 minutes and allowing the solution to cool to room temperature. When annealed 500 μL of this solution was pipetted into a CD cuvette and ran on the CD with a blank to measure against the baseline of the buffer. Measurements were recorded in triplicate with duplex's being scanned at 25 °C from 200-500 nm at a scanning rate of 20.0 nm/min and a 0.20 nm resolution.

2.6 Medaka maintenance and embryo rearing

Fish were housed in the Aquatic Omics lab with a maximum density of 2.3 cm of fish length per liter of water. To ensure genetic variety between test eggs two medaka rearing tanks were used. They were fed live brine shrimp twice daily (once in the morning, once in the afternoon) and flakes once per day (at Noon) during the breeding period. Currently, the Aquatic Omics lab at Ontario Tech University houses the wild type (wt) and d-rR-Tg(beta-actin-loxP-GFP) strains that were used in this experiment purchased from NBRP in Japan. This transgenic strain allows for the silencing of eGFP to be easily and efficiently examined after injection with siRNAs in single cell embryos. It is important to collect and inject the eggs during this period as it ensures proper siRNA distribution to each rapidly dividing cell. However, before injecting, fertilized eggs must be collected. Stage 1 embryos were obtained by placing 1 male in a tank for every one 1 female and controlling for consistent photoperiods of 14 hours of light and 10 hours of dark to simulate spring breeding conditions for optimal production. Fish breeding typically occurs immediately after light stimulation at 8: 00 am; however, it can occur up to two hours post onset. As such, the fish were monitored during this time period. After observing typical courtship behaviour which include a male sporadically chasing a female and then performing quick circling movements beneath her. If accepted the male will wrap its anal fin at the posterior of the female and she produces the oocytes which remain attached to her body during fertilization. After fertilization, the embryos can remain on the mother for a varied amount of time, approximately 24 to 48. Eggs were obtained no later than 10 minutes post fertilization to ensure they were in the single cell stage (stage 1) for injection. A net was used to catch the female medaka and hold her close to the surface of the water while

retrieving the fertilized embryos. Using a 50 ml pipette and an aspirator, the eggs were carefully and gently removed from the females' abdomens while remaining in the water to reduce stress. If the eggs could not be removed this way, the female was briefly taken out of the water and the eggs were removed from her abdomen with a finger or thumb. Once collected, the eggs were stored in a petri dish with tank water. The filaments on the embryos were removed using tweezers. The embryos were then gently rolled over P1200 sandpaper to remove any remaining debris and placed back into petri dish containing a mixture of 50% tank water and 50% rearing solution (methylene blue, NaCl, $MgS0_4$, $CaCl_2$, and KCl dissolved in MilliQ water). Finally, to ensure the eggs remained at the one cell stage for as long as possible, the petri dish was kept on ice until injection.

2.7 Injection of siRNAs into medaka embryo

Special needles were prepared from aluminosilicate glass capillaries (outside diameter 1.00 mm inside diameter 0.64 mm) using a P-97 Micropipette Puller from Sutter Instruments under these settings: Pressure = 200, Heat = 346. Pull = 30, Velocity = 120, and Time = 44 seconds. The pulled needles were snipped at the tip under a stereomicroscope using a razor blade. The needle was then backfilled with mineral oil and placed on the Drummond NanoJect III microinjector (Broomall, PA, USA). Using a HAMILTON 10 μL needle 0.5 μL of siRNA is placed on as fresh sheet of parafilm and then lining the tip of the needle with the spot of liquid the Nanoinjector is filled with injectate. It is important to perform this action slowly as any air bubbles introduced into the injector needle may cause problems such as a loss of suction when injecting. Using a plastic pipette all the collected embryos were placed at the north side of a glass petri dish rolling each individual egg to the center of the dish when ready to inject. Eggs were

manipulated using tweezers to allow the single cell of the embryo to face the injector needle perpendicularly. Finally, carefully using the right-hand micro-adjuster, the needle was inserted into the cell and the siRNA injected. Injection amounts were carried out at 8ng and 4ng of siRNA/ egg for WT/ F-siRNA-G1 and 8ng /egg for SCR-F-siRNA-G2. After injections any non-viable embryos were removed to not interfere with the results.

2.8 Light activation and inactivation of photoswitchable azobenzene siRNA

2.8.1 No light exposure (Dark) experiment

Immediately after being injected with F-siRNAs, individual embryos were transferred from a petri dish to separate wells (1 embryo per well) of a Costar 96 Well Optical Btm PolymerBase black plate by Thermofisher Scientific using a plastic pipette. Each well with an embryo was filled completely with embryo rearing solution. The plate had no light exposed to it other than natural light to determine if F-siRNA-G1 would silence as well as Wt-siRNA-G1. The eGFP of each egg was measured as stated below in section 2.9 every 24 hours for 10 days. If during this period, an embryo became non-viable the egg was removed and the previous measurements for that well were deleted from the data set for each of the light experiments.

2.8.2 Green light exposure (Azo Green) experiment

Immediately after being injected with F-siRNAs, individual embryos were placed into the wells of a black 96 well plate (one embryo per well) and exposed to green wavelength light (530 nm) using a 4.0-Watt discrete green LED wavelength 530 nm (LEDsupply) for 1 hour to inactivate the siRNA to the *cis* conformer. The embryos were approximately 14 cm away from the LED light. Due to being exposed to natural light

during each fluorescence reading every 24 hours post injection (hpi) the embryos were re-exposed to the same green light.

2.8.3 Green to Blue light exposure (Azo Green/Blue @72) experiment

Immediately after being injected with F-siRNAs, individual embryos were placed in the wells of a black 96 well plate and exposed to green wavelength light (530 nm) for 1 hour to inactivate the siRNA to the *cis* conformer. After each eGFP reading every 24 hpi the embryos were re-exposed to the same green wavelength light until 72 hpi when the embryos were then exposed to a blue light every 24 hours using a 4.0- Watt blue LED (LEDsupply) 470 nm (+/- 5 nm) wavelength to reactivate the siRNA to the *trans* conformer.

2.8.4 Blue to Green light exposure (Azo Blue/Green @72) experiment

Immediately after being injected with F-siRNAs, individual embryos were placed in the wells of a black 96 well plate and exposed to blue wavelength light (470 nm) for 1 hour to activate the siRNA to the *trans* conformer. After each eGFP reading every 24 hpi the embryos were re-exposed to the same blue wavelength light until 72 hpi when the embryos were then exposed to a green light every 24 hours (530 nm) inactivating the siRNA to the *cis* conformer.

2.9 eGFP fluorescence measurements

Measurements of fluorescence were taken using a BioTek CytationGen5 plate reader by Agilent with expression being quantified in relative fluorescence units (RFU). Each embryo had to be centered in a 96 well plate using a tweezer to detect optimal fluorescence with a read height of 8.00 nm. The detection method was set to absorbance,

read type was set to endpoint kinetic, and optic was set on monochromators. The exposure was kept to a minimum for each run to ensure a baseline between embryos and the specific fluorophore used was eGFP. To eliminate autofluorescence, unmodified wild type medaka embryos fluorescence was measured at each time point and subtracted.

2.10 Statistical analysis

Statistical analysis was performed using GraphPad Prism 10. Data is represented at mean ± s.d. Values in figures are reported as eGFP fluorescence as a % of our control denoted as a red dotted line (noninjected embryos). A Two-way ANOVA with a Tukey's post hoc test was used to compare each light treatment to one another with an emphasis on comparing them back to the control within the same time point. An additional repeated measures Two-way ANOVA with a post hoc Tukey's test was conducted to compare each light treatment to the same light treatment at a different time point.

Chapter 3: Results and Discussion

3.1 Chemical synthesis analysis

3.1.1 Analysis for 4-bromo-2,6-difluoroaniline (compound 2)

Three syntheses for reaction 1 (synthesis of 4-bromo-2,6-difluoroaniline) were performed to ensure an adequate amount of starting material. The first attempt resulted in a low yield (35%), as the crude product was not split into two portions when performing column chromatography and a dry load column was not used. Due to the large amount of crude product, a dry load allows for a higher yield of purified product to be obtained by first binding our product to silica in a rotary evaporator and then splitting the portion in half to run the column twice. This method led to a much higher yield (60 %), with the third and final synthesis having the highest yield (91%).

3.1.2 Analysis for 4-amino-3,5-difluorobenzonitrile (compound 3)

The synthesis of 4-amino-3,5-difluorobenzonitrile was performed seven times due to many attempts resulting in low yields (5 to 20 % for the first three reactions). This was most likely due to losing a large amount of product in an emulsion that formed consistently during the extraction step of the work up. To prevent this loss of product, a number of strategies were implemented. First, a large volume of water and ethyl acetate was used during the extraction step, approximately 500 ml of each. This led to a smaller emulsion forming and thus the reaction work up was easier to perform. The second technique implemented was to use a concentrated NaCl water solution during the extraction which, when done with the first preventive measure, led to almost no emulsion forming. Another problem leading to a low yield was that the purified material coming from the column was

a clear and colourless solution. However, when using a UV flashlight, the molecule could be tracked throughout the column to observe when the product was eluting

3.1.3 Analysis for 4-amino-3,5-difluorobenzoic acid (compound 4)

The synthesis of 4-amino-3,5-difluorobenzoic acid was fairly straight forward and was performed five times to have a large stockpile of compound 4. Each reaction led to a yield above 80% most likely due to there being no final purification step after precipitation of the product from high acidic conditions.

3.1.4 Analysis for 4-amino-N-(2-((tert-Butyldimethylsilyl)oxy)ethyl)-3,5-difluorobenzamide (compound 5)

The synthesis of 4-amino-N-(2-((tert-Butyldimethylsilyl)oxy)ethyl)-3,5-difluorobenzamide was performed two times. The first attempt had a low yield due to overloading the thick viscous crude product in the column. When separating the crude product into two equal portions, the column became much more manageable, and the yield increased significantly from 43% to 85%.

3.1.5 Analysis for (E)-4,4'-(diazene-1,2-diyl) bis(N-(2-(tert-butyldimethylsilyl)oxy)ethyl)-3,5-difluorobenzamide (compound 6)

The synthesis of (E)-4,4'-(diazene-1,2-diyl) bis(N-(2-(tert-butyldimethylsilyl)oxy)ethyl)-3,5-difluorobenzamide was performed three times. A challenge encountered during the second reaction attempt was the formation of a precipitate when loading the column. This precipitate blocked the flow of air throughout the column, thus slowing down product elution. Additionally, due to having a *trans* and *cis* form, it is possible to get two separate product spots with slightly different Rf values, as each conformer has a different polarity.

3.1.6 Analysis for (E)-4,4'-(diazene-1,2-diyl) bis(3,5-difluoro-N-(2-hydroxyethyl)benzamide (compound 7)

The synthesis of (E)-4,4'-(diazene-1,2-diyl) bis(3,5-difluoro-N-(2-hydroxyethyl)benzamide was performed once at a large scale. The deprotection of the TBS group did not require any further purification after extracting out unreacted starting material and OH-TBS. Due to this, unlike the prior reactions, this reaction needed to be conducted under argon gas to ensure no impurities formed.

3.1.7 Analysis for (E)-N-(2-(bis(4-methoxyphenyl)(phenyl)methoxy)ethyl)-4-((2,6-difluoro-4-((2-hydroxyethyl)carbamoyl)phenyl)diazenyl)-3,5 difluorobenzamide (compound 8)

The synthesis of compound 8 was performed five times due to obtaining low yields in the first three attempts. The low yield most likely occurred due to the DMT group becoming unstable and leaving the desired product on the acidic silica column. Like reaction five (3.1.5), precipitates would sometimes form when loading the column, slowing down the purification and allowing for the degradation of the desired product. To counteract this, the percentage of methanol used was increased from 5 % to 10 %.

3.1.8 Analysis for E)-2-(4-((4-((2-(bis(4-methoxyphenyl)(phenyl) methoxy) ethyl)carbamoyl)-2,6-difluorophenyl)diazenyl) 3,5difluorobenzamido) ethyl (2-cyanoethyl) diisopropylphosphoramidite (compound 9)

The synthesis of compound 9 was performed four times with only one successful attempt. There are a variety of challenges to overcome when completing a phosphoramidite reaction such as making sure there is absolutely no water in the reaction and performing the purification step quickly. One water molecule can disrupt the entire reaction and the phosphoramidite is very sensitive so the column must be performed quickly. The first three attempts showed no ^{31}P peak in the NMR spectra indicating the reaction did not occur.

3.2 Fluorescence variation of treatments over time

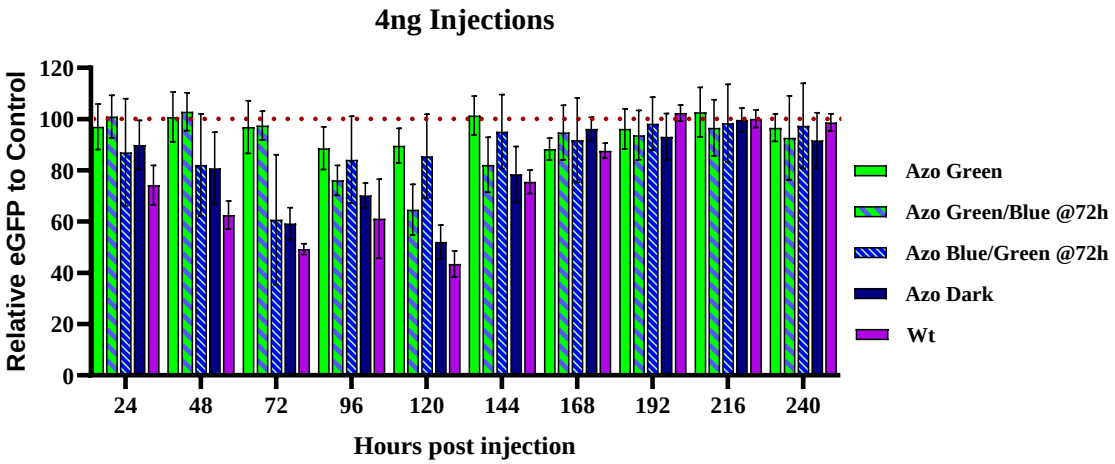

Figure 3.1 – Normalized enhanced green fluorescent protein expression for F-siRNA-g1 and Wt-siRNA-g1 at 4 ng in Japanese medaka embryos 24 - 240 hpi. Azo Green corresponds to the siRNA being exposed to green 530 nm wavelength light at 0 hpi every 24 hours (n=3). Azo Green/Blue (G/B) @72 h corresponds to exposing the eggs at 0, 24 and 48 hpi to green light; however, at 72 hpi the eggs were exposed to 470 nm blue wavelength light every 24 hours (n=5). Azo Blue/Green (B/G) @72 h corresponds to the eggs being exposed to blue light at 0, 24 and 48 hpi; however, at 72 hpi the eggs were exposed to green light every 24 hours (n=8). Azo Dark corresponds to embryos being injected with F-siRNA and kept in the dark (n=6). Wt corresponds to embryos being injected with Wt-siRNA (n=9).

There was no statistically significant variance in fluorescence of the GLT embryos (Azo Green) (Repeated measures Two-way ANOVA, Tukey's test, $P < 0.05$) which concurs with the trend of the bars between the 24 to 240-hour time period. This strongly supports that the azobenzene molecular switch was in the off position after the green light exposure and thus minimal siRNA activity was occurring. Notably, when compared to the control data, the GLT embryos have slightly lower fluorescence suggesting not all the F-siRNA remain in the *cis* off position.

The trend of the green light to blue light experiment in figure 3.1, (Azo G/B @72), implies a photo-switch did occur as after the 72 hpi time point a drop in fluorescence is shown at 96 hpi. However, the results of the Two-way ANOVA indicate no significant

drop between these data points; but there is a significant drop in fluorescence between 72 hpi and 120 hpi in the green to blue light experiment with 4 ng of F-siRNA. This demonstrates that siRNA gene silencing is activated by blue light exposure, though it required 48 hours for the eGFP silencing to cause a statistically significant and observable effect. This is further reinforced by the results from the 8 ng injections, for which there was a similar statistical result after 48 hours (**Figure 3.2)**. One explanation for differences in fluorescence between 72 hpi to 96 hpi from both the 4 ng and 8 ng injections may be due to the actual life cycle of the embryo. Between this time period the embryo goes from stage 29 to stage 32 with significant growth development occurring within each.[33,39] For example, throughout this 24-hour period the sinus venosus, atrium, ventricle, and bulbus arteriosus all become differentiated allowing blood to start circulating the body while the brain and liver become pronounced enough to be identified.[33] Additionally, the tail elongates due to muscle development to prepare for hatching.[33,39] Due to the considerable growth and development of the embryo during this stage a substantial increase in eGFP expression should also occur as these Tg medaka are designed to produce eGFP with organ development. Therefore, this substantial increase in eGFP production compounded with the fact that RNAi takes time to activate, may be the reason why a significant decrease in fluorescence occurs after 120 hpi and why the effect lasts longer with the larger injection mass[1]. After this period fluorescence steadily returns to baseline indicating the F-siRNA may be entirely used up or destroyed through enzymatic degradation.

When evaluating the blue to green light treated eggs (Azo B/G @72) there is a clear silencing effect during the first 72 hpi (similar to the Azo dark experiment). The green light was introduced at the 72 hpi timepoint, and the fluorescence significantly increased 48

hours afterward (Two-way ANOVA, Tukey's test, $P < 0.05$). Like the previous experiment this suggests 48 hours after a change in light treatment a significant difference in fluorescence can be seen which indicates a photoswitch occurred turning the F-siRNA off.

We observed a steady decline in fluorescence in the Azo Dark experiment until the 120 hpi time point after which fluorescence starts to progressively increase. This was supported by the results of the ANOVA analysis, with a significant decrease in expression from 48 hpi to 72 hpi (Two-way ANOVA, Tukey's test, $P < 0.05$). Fluorescence then marginally (but not significantly) increased from 72 hpi to 96 hpi (most likely due to the proposed reason above). After this, there is a significant increase in fluorescence from 120 hpi to 144 hpi, suggesting the siRNA has been used completely or has been degraded by a nuclease enzyme. The trends associated with this experiment closely resemble the Wt siRNA data, however the Wt siRNA was slightly more effective at silencing, which is to be expected as the F-azobenzene modifications has been shown to slightly decrease silencing potential.[29] In general, these observations are consistent with previous data when measuring luciferase in an in vitro cell line.

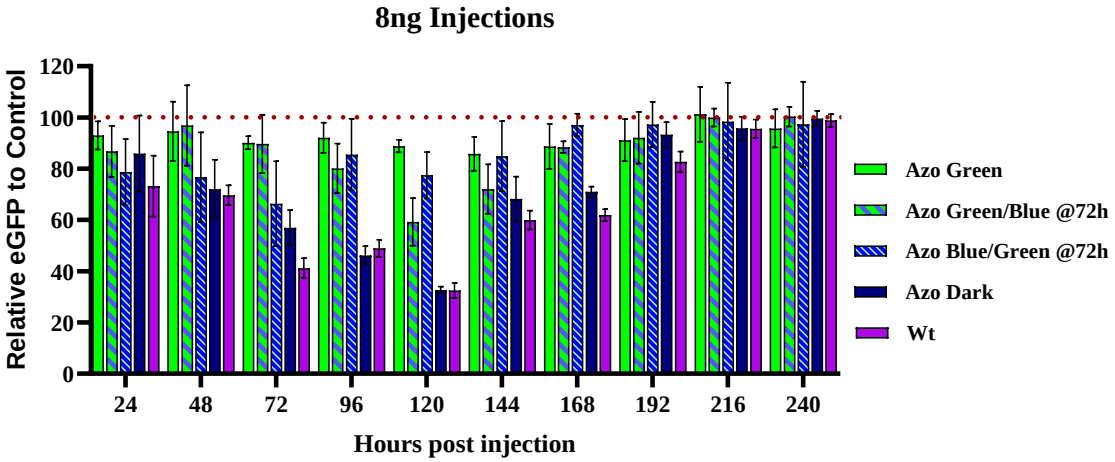

Figure 3.2 – Normalized enhanced green fluorescent protein expression for F-siRNA-g1 and Wt-siRNA-g1 at 8 ng in Japanese medaka embryos 24 - 240 hpi. Azo Green corresponds to the siRNA being exposed to green 530 nm wavelength light at 0 hpi every 24 hours (n=5). Azo G/B @72 h corresponds exposing the eggs at 0, 24 and 48 hpi to green light; however, at 72 hpi the eggs were exposed to 470 nm blue wavelength light every 24 hours (n=7). Azo B/G @72 h corresponds to the eggs being exposed to blue light at 0, 24 and 48 hpi; however, at 72 hpi the eggs were exposed to green light every 24 hours (n=8). Azo Dark corresponds to embryos being injected with F-siRNA kept in the dark (n=7). Wt corresponds to embryos being injected with Wt-siRNA (n=12).

Again, there was no statistical variance in GLT embryos between the 24 to 240-hour time period for the 8 ng injected embryos. This observation suggests that the azobenzene molecular switch was in the off position due to green light exposure for the duration of this experiment, and thus minimal siRNA activity occurred. Like the 4 ng injections, the GLT embryos have slightly lower fluorescence compared to the control eggs, suggesting not all the F-siRNA remain in the *cis* off position.

Similarly, to the 4 ng experiments, the Azo G/B @72, indicates a photo-switch did occur after the 72 hpi time point, which was observed as a mild drop in fluorescence at 96 hpi, and then a significant drop in fluorescence after 120 hpi, which demonstrates how the molecular switch can be turned on and off again through blue light and green light respectively, although observable effects take time. After 120 hpi, fluorescence starts to steadily increase, which is in agreement with our other findings.

When evaluating the 8 ng Azo B/G @72 injected eggs it is clear that there is a silencing effect during the first 72 hpi, until which point the embryos were exposed to green light, and then fluorescence significantly increases 24 hours later at 96 hpi (Figure 3.2). In contrast, a 48-hour period was needed to significantly increase eGFP fluorescence in the embryos injected with 4 ng F-siRNA. This was in opposition to the hypothesized effect, where a higher dose would cause greater silencing, and thus when the F-siRNA is switched off at the 72-hour mark, a lower increase in fluorescence. This could be an indication that RISC loading had reached its limit around 4 ng of siRNA in the medaka embryos and thus an 8 ng dose was in excess.[40]

In the 8 ng Azo Dark experiment, there was a statistically significant decline in fluorescence until the 120 hpi time point, after which fluorescence progressively increased (Two-way ANOVA, Tukey's test, $P < 0.05$). This was likely due to the siRNA being completely consumed or degraded by an enzyme. The observations from this experiment closely resemble the Wt siRNA data, however with Wt siRNA having better silencing. This is an expected result observed in our previous F-siRNA data in HeLa cells.[29]

3.3 Fluorescence variation between treatments

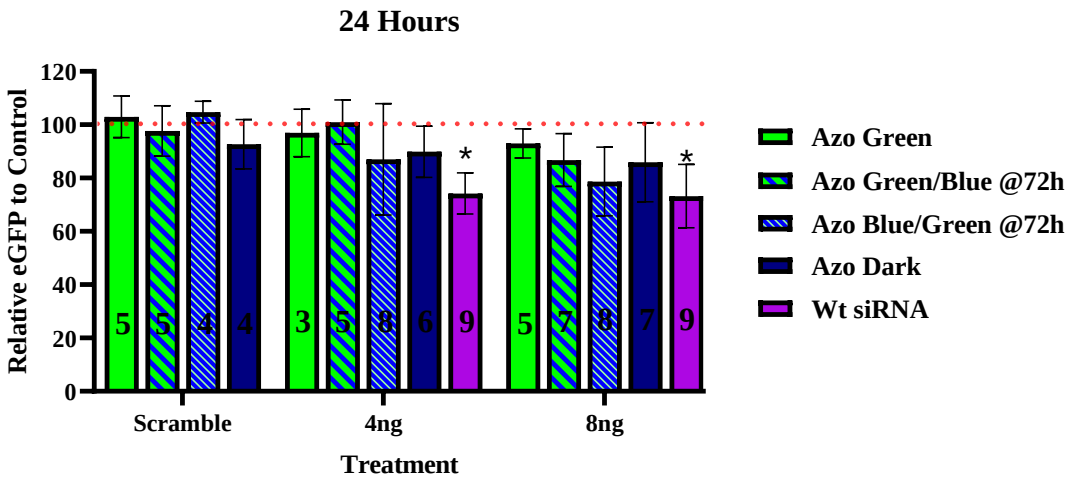

Figure 3.3 – Normalized enhanced green fluorescent protein expression for F-siRNA-g1, Wt-siRNA-g1 (4ng and 8ng), and SCR-F-siRNA-g2 (8ng) in Japanese medaka embryos at 24 hpi. Azo Green corresponds to the siRNA being exposed to green 530 nm wavelength light at 0 hpi every 24 hours. Azo G/B @72 h corresponds exposing the eggs at 0, 24 and 48 hpi to green light; however, at 72 hpi the eggs were exposed to 470 nm blue wavelength light. Azo B/G @72 h corresponds to the eggs being exposed to blue light at 0, 24 and 48 hpi; however, at 72 hpi the eggs were exposed to green light. Azo Dark corresponds to embryos being injected with F-siRNA and exposed to natural light. Wt corresponds to embryos being injected with Wt-siRNA. The numbers on the bars denote the sample size. (n value)

As expected, the SCR-CRTL (SCR-F-siRNA-g2) data were nearly equivalent to the control levels of eGFP expression at 24 hpi (Two-way ANOVA, Tukey's test, $P < 0.05$). In accordance with this result both the 4 and 8 ng GLT (Azo Green) eggs show no knockdown at this time point. For both the 4 and 8 ng injections there was no statistical difference in fluorescence from green to blue light treated (Azo G/B @72 h) eggs when compared to the control, which makes sense as at this time point, they are exactly the same as GLT eggs. Notably, although there is a downward dose-dependent trend for the BLT embryos there is no significant decrease which also occurred in the Azo Dark treatment eggs. Finally, the positive control Wt siRNA caused significant dose-dependent silencing at this time point when compared to the control.

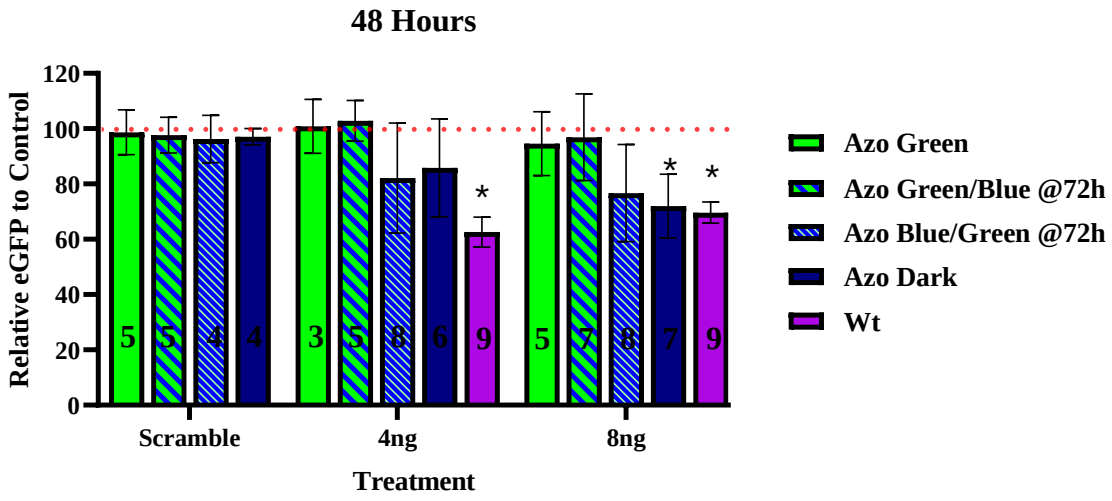

Figure 3.4 – Normalized enhanced green fluorescent protein expression for F-siRNA-g1, Wt-siRNA-g1, and SCR-F-siRNA-g2 at 4 and 8 ng in Japanese medaka embryos 48 hpi. Azo Green corresponds to the siRNA being exposed to green 530 nm wavelength light at 0 hpi every 24 hours. Azo G/B @72 h corresponds exposing the eggs at 0, 24 and 48 hpi to green light; however, at 72 hpi the eggs were exposed to 470 nm blue wavelength light every 24 hours. Azo B/G @72 h corresponds to the eggs being exposed to blue light at 0, 24 and 48 hpi; however, at 72 hpi the eggs were exposed to green light every 24 hours. Azo Dark corresponds to embryos being injected with F-siRNA and exposed to natural light. Wt corresponds to embryos being injected with Wt-siRNA. The numbers on the bars denote the sample size. (n value)

As expected, each of SCR-control siRNA-treated embryos had the same levels of eGFP expression at 48 hpi as the control (Two-way ANOVA, Tukey's test, $P < 0.05$). Both concentrations showed no knockdown for Azo green, Azo G/B @72h and Azo B/G @72h treated eggs. Both concentrations of F-siRNA exposed to no light (Azo dark) depict decreasing fluorescence however only the 8 ng showed a significant decrease from the control, which may indicate dose-dependence at the 48-hour time point. In contrast, both concentrations of Wt siRNA produced a significant drop in eGFP expression with the 4 ng injected eggs showing a slight increase in silencing.

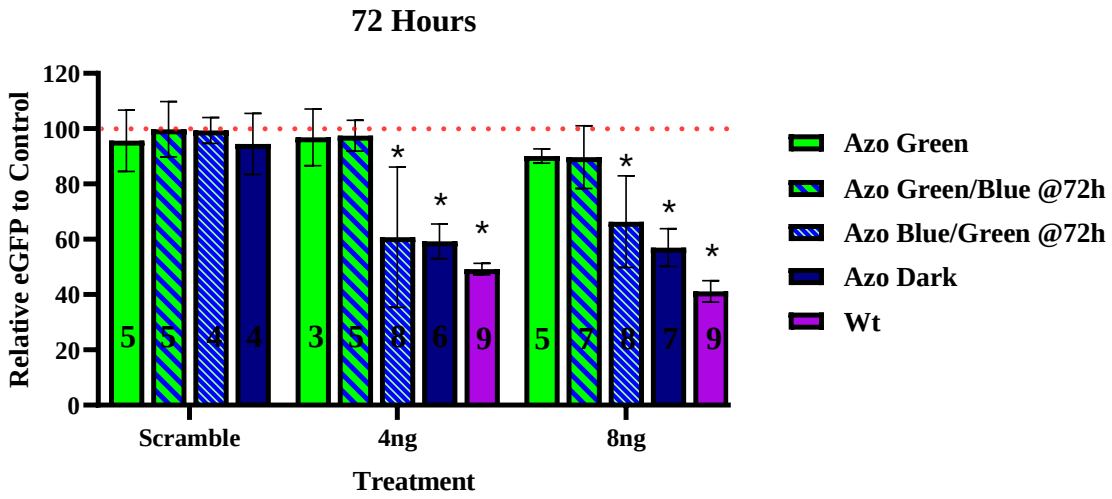

Figure 3.5 – Normalized enhanced green fluorescent protein expression for F-siRNA-g1, Wt-siRNA-g1, and SCR-F-siRNA-g2 at 4 and 8 ng in Japanese medaka embryos 72 hpi. Azo Green corresponds to the siRNA being exposed to green 530 nm wavelength light at 0 hpi every 24 hours. Azo G/B @72 h corresponds exposing the eggs at 0, 24 and 48 hpi to green light; however, at 72 hpi the eggs were exposed to 470 nm blue wavelength light every 24 hours. Azo B/G @72 h corresponds to the eggs being exposed to blue light at 0, 24 and 48 hpi; however, at 72 hpi the eggs were exposed to green light every 24 hours. Azo Dark corresponds to embryos being injected with F-siRNA and exposed to natural light. Wt corresponds to embryos being injected with Wt-siRNA. The numbers on the bars denote the sample size. (n value)

Comparing the fluorescence measurements from the scramble controls, green light (Azo green), and green to BLT (Azo G/B @72h) embryos at 72 hpi, no knockdown occurred when compared to the control. When comparing the blue light to GLT (Azo B/G @ 72h) eggs there was significant eGFP silencing for both the 4 and 8 ng injections, which makes sense as these were only exposed to blue light at this timepoint (Two-way ANOVA, Tukey's test, $P < 0.05$). There was no statistical difference when comparing these embryos to no light (Azo Dark) F-siRNA fluorescence for both concentrations. There was a significant difference between the fluorescence of Azo B/G, Azo dark and Wt embryos when individually compared to Azo green embryos, further reinforcing that the activated F-siRNAs silenced eGFP expression. This clearly demonstrates that the blue light treatment caused silencing while the green light treatment removed the effect of silencing.

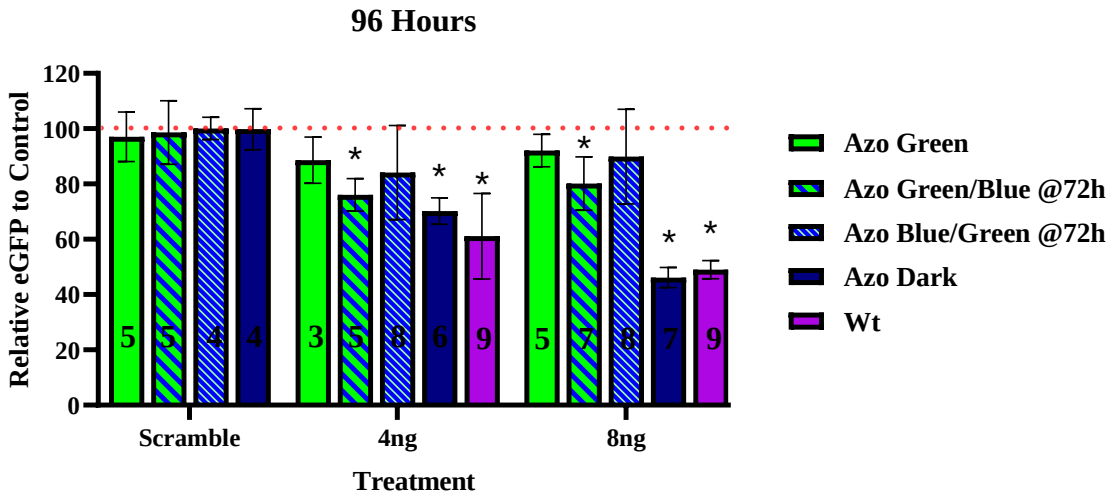

Figure 3.6 – Normalized enhanced green fluorescent protein expression for F-siRNA-g1, Wt-siRNA-g1, and SCR-F-siRNA-g2 at 4 and 8 ng in Japanese medaka embryos 96 hpi. Azo Green corresponds to the siRNA being exposed to green 530 nm wavelength light at 0 hpi every 24 hours. Azo G/B @72 h corresponds exposing the eggs at 0, 24 and 48 hpi to green light; however, at 72 hpi the eggs were exposed to 470 nm blue wavelength light every 24 hours. Azo B/G @72 h corresponds to the eggs being exposed to blue light at 0, 24 and 48 hpi; however, at 72 hpi the eggs were exposed to green light every 24 hours. Azo Dark corresponds to embryos being injected with F-siRNA and exposed to natural light. Wt corresponds to embryos being injected with Wt-siRNA. The numbers on the bars denote the sample size. (n value)

All scramble controls along with both concentrations of GLT eggs had no drop in fluorescence when compared to the control at 96 hpi. After being exposed to blue light 24 hours prior, the Azo G/B @72h had a decrease in fluorescence and showed a significant difference in fluorescence from the control. However, the effect was not affected by dose, as the 8 ng injected embryos were marginally higher than the 4 ng ones. After being exposed to green light 24 hours prior (Azo B/G @72h), an increase in fluorescence was observed for both injection amounts with each concentration being statistically similar to the control (Two-way ANOVA, Tukey's test, $P < 0.05$). Both the Azo Dark and Wt siRNA embryos had a significant decrease in fluorescence compared to the control, indicating silencing was still in effect.

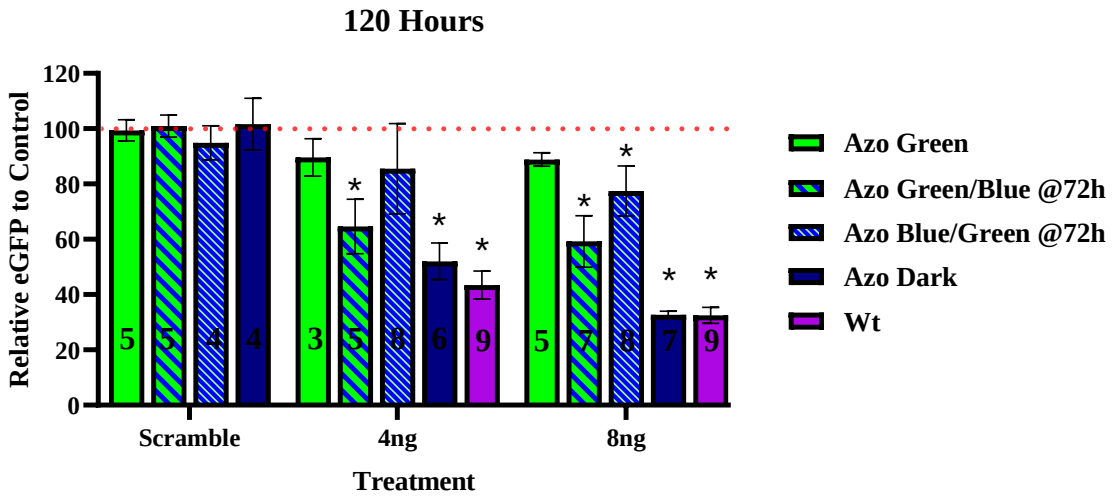

Figure 3.7 – Normalized enhanced green fluorescent protein expression for F-siRNA-g1, Wt-siRNA-g1, and SCR-F-siRNA-g2 at 4 and 8 ng in Japanese medaka embryos 120 hpi. Azo Green corresponds to the siRNA being exposed to green 530 nm wavelength light at 0 hpi every 24 hours. Azo G/B @72 h corresponds exposing the eggs at 0, 24 and 48 hpi to green light; however, at 72 hpi the eggs were exposed to 470 nm blue wavelength light every 24 hours. Azo B/G @72 h corresponds to the eggs being exposed to blue light at 0, 24 and 48 hpi; however, at 72 hpi the eggs were exposed to green light every 24 hours. Azo Dark corresponds to embryos being injected with F-siRNA and exposed to natural light. Wt corresponds to embryos being injected with Wt-siRNA. The numbers on the bars denote the sample size. (n value)

At time point 120 hpi, the SCR controls and GLT eggs showed no fluorescence silencing. However, fluorescence silencing remained in Azo G/B treated embryos at both concentrations when compared to the control (Two-way ANOVA, Tukey's test, $P < 0.05$). This indicates that F-siRNA gene suppression was activated after exposure to blue light at 72 hpi. Further evidence of the switch working is the fact that there is a difference in fluorescence when comparing GLT to Azo G/B eggs. Both concentrations of Azo B/G had no statistical difference in fluorescence compared to the control. This also supports the fact that the F-siRNA can be turned off *in vivo* with green light. This is further strengthened by the fact that when compared to the GLT data, there is no statistical difference; but when compared to the Azo Dark embryos there is. Finally, when assessing the fluorescence of Azo G/B compared to Azo B/G there is a variation, where the G/B fluorescence was lower.

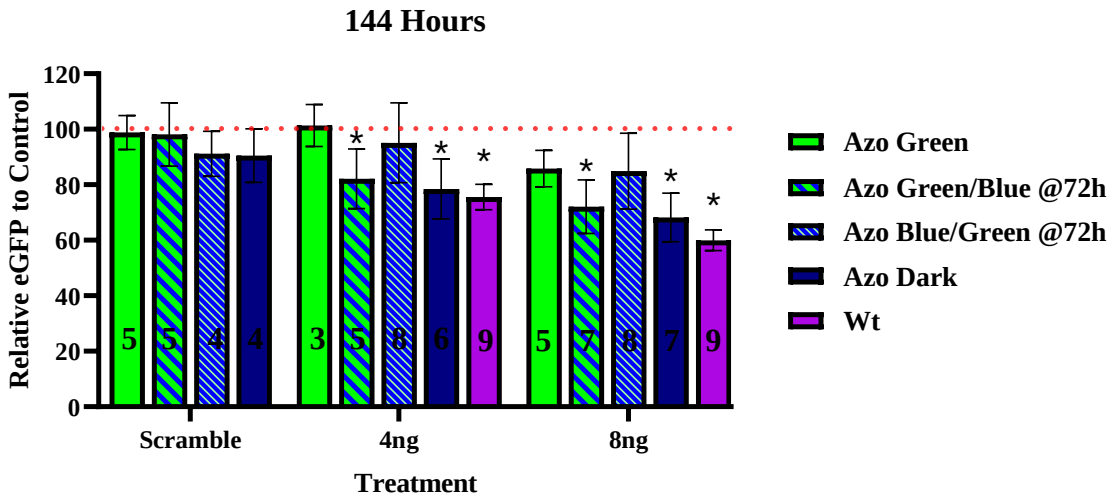

Figure 3.8 – Normalized enhanced green fluorescent protein expression for F-siRNA-g1, Wt-siRNA-g1, and SCR-F-siRNA-g2 at 4 and 8 ng in Japanese medaka embryos 144 hpi. Azo Green corresponds to the siRNA being exposed to green 530 nm wavelength light at 0 hpi every 24 hours. Azo G/B @72 h corresponds exposing the eggs at 0, 24 and 48 hpi to green light; however, at 72 hpi the eggs were exposed to 470 nm blue wavelength light every 24 hours. Azo B/G @72 h corresponds to the eggs being exposed to blue light at 0, 24 and 48 hpi; however, at 72 hpi the eggs were exposed to green light every 24 hours. Azo Dark corresponds to embryos being injected with F-siRNA and exposed to natural light. Wt corresponds to embryos being injected with Wt-siRNA. The numbers on the bars denote the sample size. (n value)

At time point 144 hpi the SCR controls and GLT eggs show no fluorescence silencing. Additionally, the G/B treatment data shows an increase in fluorescence from the 120 hpi graph; however, they are still significantly different from the control (Two-way ANOVA, Tukey's test, $P < 0.05$). This implies the F-siRNA has either been depleted or degraded while the embryos start expressing control levels of eGFP. Another indication that this is the case is that G/B and B/G are not statistically different from one another thus suggesting even after being exposed to blue light silencing is no longer occurring. To further back this claim when comparing just B/G to the control they are statistically similar. Both Azo dark and Wt embryos have less fluorescence when compared to the control; however, they have increased from the 120 hpi time point.

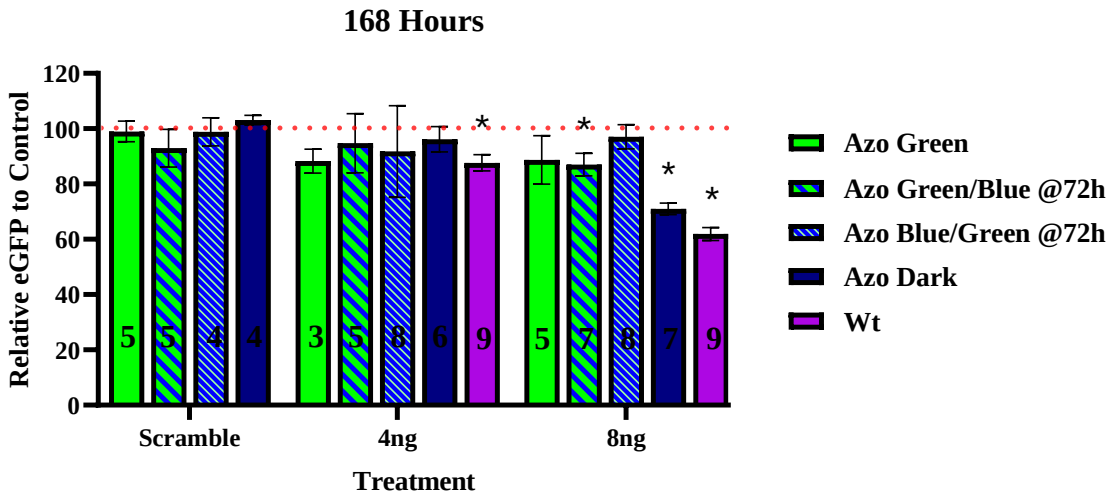

Figure 3.9 – Normalized enhanced green fluorescent protein expression for F-siRNA-g1, Wt-siRNA-g1, and SCR-F-siRNA-g2 at 4 and 8 ng in Japanese medaka embryos 168 hpi. Azo Green corresponds to the siRNA being exposed to green 530 nm wavelength light at 0 hpi every 24 hours. Azo G/B @72 h corresponds exposing the eggs at 0, 24 and 48 hpi to green light; however, at 72 hpi the eggs were exposed to 470 nm blue wavelength light every 24 hours. Azo B/G @72 h corresponds to the eggs being exposed to blue light at 0, 24 and 48 hpi; however, at 72 hpi the eggs were exposed to green light every 24 hours. Azo Dark corresponds to embryos being injected with F-siRNA and exposed to natural light. Wt corresponds to embryos being injected with Wt-siRNA. The numbers on the bars denote the sample size. (n value)

Statistical analysis of the SCR control data shows that each of treated embryos continues to show control levels of eGFP expression after 168 hours. In accordance with this result both the 4 and 8 ng GLT eggs show no knockdown at this time point which concurs with the previous statistical test in which no silencing occurred across each time point. For each of the 4 ng injected embryos all statistical analysis demonstrates control levels of expression except for the Wt treatment. This makes sense as the Wt-siRNA has consistently shown the greatest knockdown effect. For the 8 ng injected embryos G/B, Azo Dark and Wt still remain different from control levels of fluorescence (Two-way ANOVA, Tukey's test, $P < 0.05$)

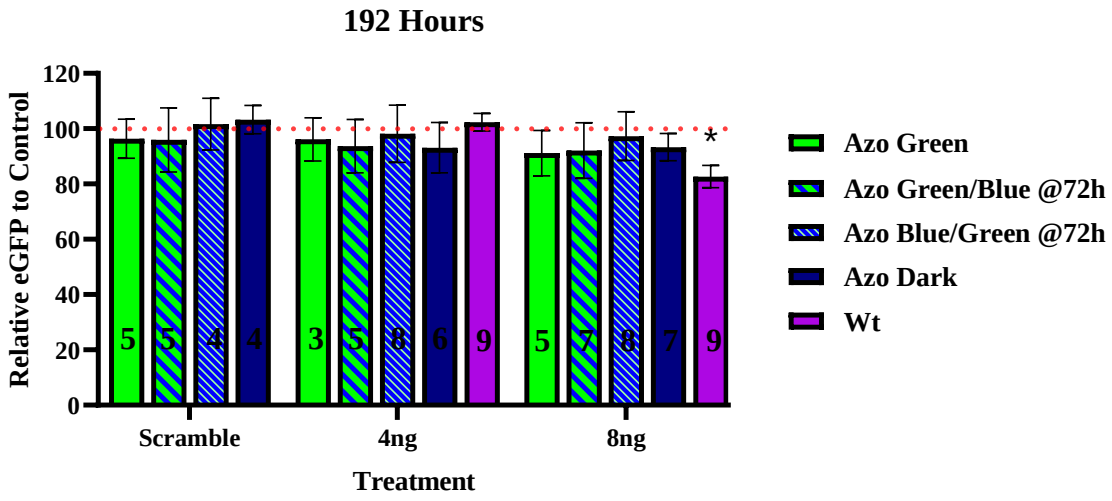

Figure 3.10 – Normalized enhanced green fluorescent protein expression for F-siRNA-g1, Wt-siRNA-g1, and SCR-F-siRNA-g2 at 4 and 8 ng in Japanese medaka embryos 192 hpi. Azo Green corresponds to the siRNA being exposed to green 530 nm wavelength light at 0 hpi every 24 hours. Azo G/B @72 h corresponds exposing the eggs at 0, 24 and 48 hpi to green light; however, at 72 hpi the eggs were exposed to 470 nm blue wavelength light every 24 hours. Azo B/G @72 h corresponds to the eggs being exposed to blue light at 0, 24 and 48 hpi; however, at 72 hpi the eggs were exposed to green light every 24 hours. Azo Dark corresponds to embryos being injected with F-siRNA and exposed to natural light. Wt corresponds to embryos being injected with Wt-siRNA. The numbers on the bars denote the sample size. (n value)

By the 192 hpi time point, only the 8 ng Wt RNA treated embryos remain statistically different from control levels of fluorescence. This is likely because each F-siRNA has either been degraded or consumed. At the 216 hpi time point, (Figure 3.11) each treatment is not significantly different to the control and to each other (Two-way ANOVA, Tukey's test, $P < 0.05$). At the 240 hpi time point, (Figure 3.12) each treatment is significantly no different to not only the control but also to each other (Two-way ANOVA, Tukey's test, $P < 0.05$).

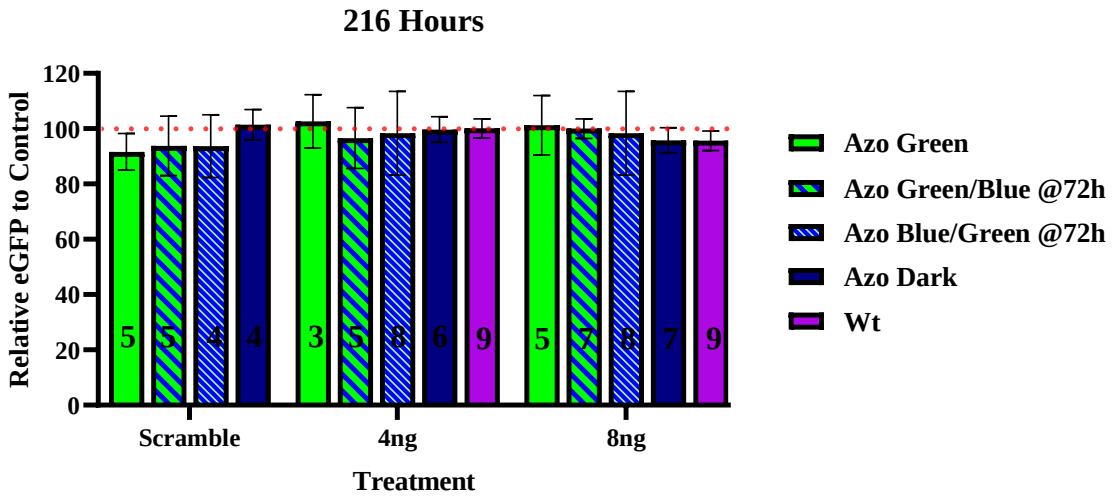

Figure 3.11 – Normalized enhanced green fluorescent protein expression for F-siRNA-g1, Wt-siRNA-g1, and SCR-F-siRNA-g2 at 4 and 8 ng in Japanese medaka embryos 216 hpi. Azo Green corresponds to the siRNA being exposed to green 530 nm wavelength light at 0 hpi every 24 hours. Azo G/B @72 h corresponds exposing the eggs at 0, 24 and 48 hpi to green light; however, at 72 hpi the eggs were exposed to 470 nm blue wavelength light every 24 hours. Azo B/G @72 h corresponds to the eggs being exposed to blue light at 0, 24 and 48 hpi; however, at 72 hpi the eggs were exposed to green light every 24 hours. Azo Dark corresponds to embryos being injected with F-siRNA and exposed to natural light. Wt corresponds to embryos being injected with Wt-siRNA. The numbers on the bars denote the sample size. (n value)

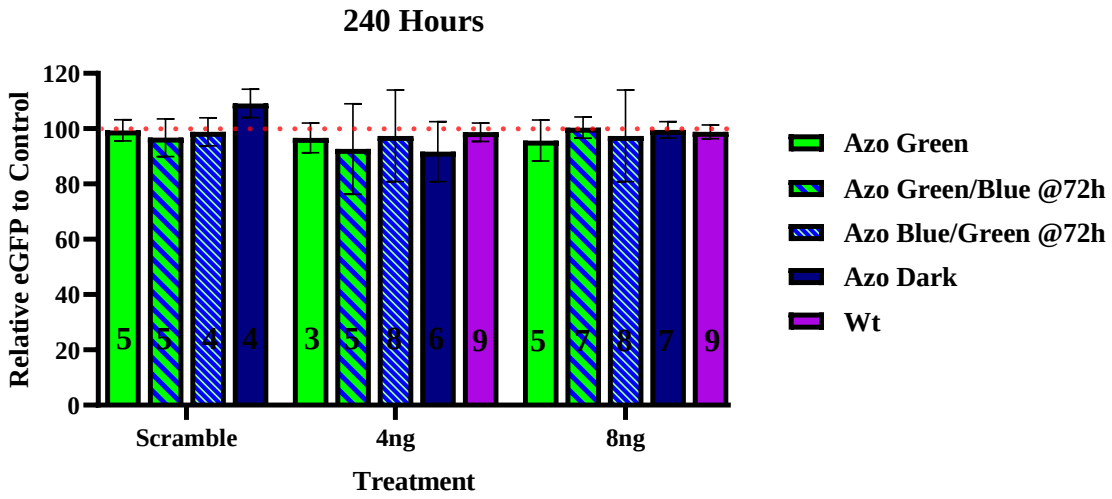

Figure 3.12 – Normalized enhanced green fluorescent protein expression for F-siRNA-g1, Wt-siRNA-g1, and SCR-F-siRNA-g2 at 4 and 8 ng in Japanese medaka embryos 240 hpi. Azo Green corresponds to the siRNA being exposed to green 530 nm wavelength light at 0 hpi every 24 hours. Azo G/B @72 h corresponds exposing the eggs at 0, 24 and 48 hpi to green light; however, at 72 hpi the eggs were exposed to 470 nm blue wavelength light every 24 hours. Azo B/G @72 h corresponds to the eggs being exposed to blue light at 0, 24 and 48 hpi; however, at 72 hpi the eggs were exposed to green light every 24 hours. Azo Dark corresponds to embryos being injected with F-siRNA and exposed to natural light. Wt corresponds to embryos being injected with Wt-siRNA. The numbers on the bars denote the sample size. (n value)

3.4 Silencing ability of F-siRNAs compared to control levels

The embryo images (**Figure 3.13)**, taken using the Cytation5 plate reader, show a clear difference in green pigmentation (representing the expression of eGFP) when comparing the control embryos to the 8 ng injected embryos at 48 hpi to 168 hpi. Overall, this is the anticipated result, especially when looking at the statistical and graphical data. It should be noted that even though the 4 ng injections show a drop when measuring fluorescence, there was no difference in the physical image when compared to control embryos. (Data not shown)

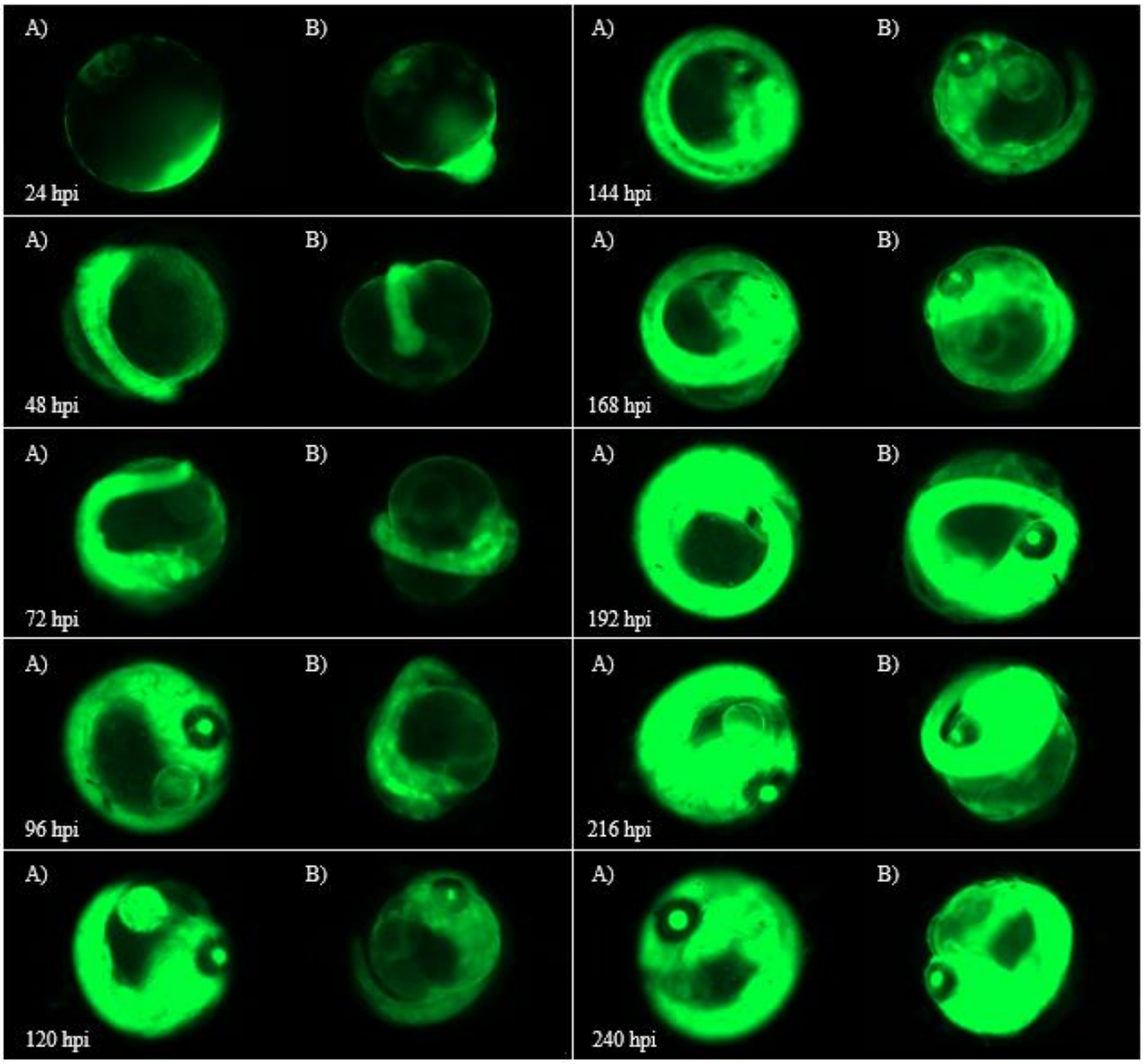

Figure 3.13 – A) Images of control Japanese Medaka embryos vs B) embryos injected with 8ng of F-siRNA-G1 kept in the dark (Azo Dark right) from 24 to 240 hpi.

The purpose of the Azo dark experiment had two goals. First to demonstrate that our F-siRNAs could silence eGFP in Tg Japanese medaka embryos. Second, if they could act as effective gene suppressors how comparable would this be to Wt naked siRNA. From the data collected it appears that the first goal was a success and F-siRNAs when kept under natural light can act to supress genes *in-vivo.* This is a step beyond our previous work which had only shown silencing in HeLa cells.[29] Furthermore, as previously shown F-siRNAs silence eGFP somewhat less effectively than Wt siRNA, but still with high potency.

3.5 Inactivation of F-siRNA from green light treatment

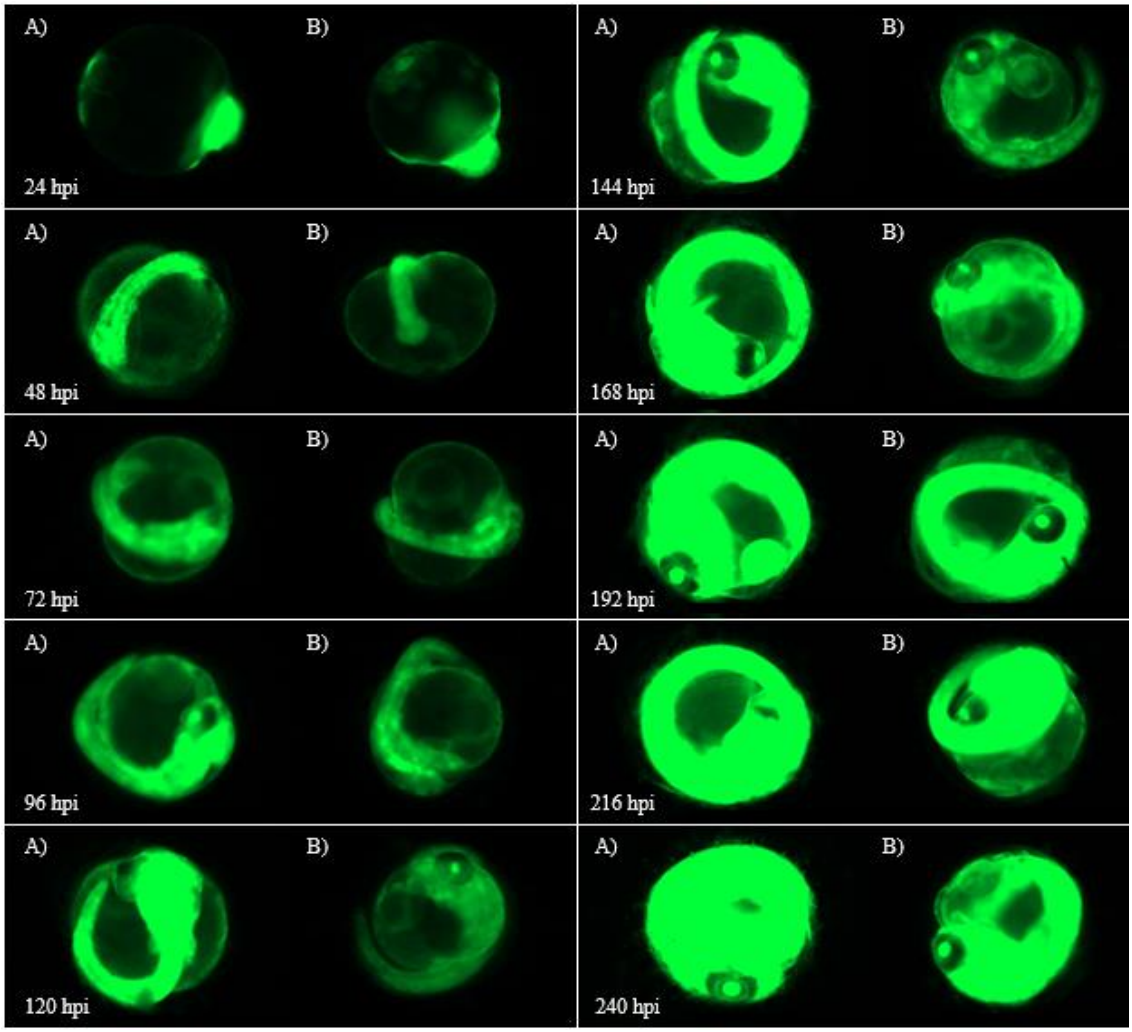

Figure 3.14 – A) Images of Japanese Medaka embryos injected with 8ng of F-siRNA-G1 held under green light (Azo Green) vs B) dark conditions (Azo Dark) from 24 to 240 hpi.

The images above (in Figure 3.14) show a clear disruption in eGFP fluorescence between embryos exposed to green light and no light on the left and right respectively around 72 hpi, when it is clear to see the embryo on the right has a less vibrant green colour which continues until 168 hpi. This not only highlights the silencing effect of embryos left in the dark, but also demonstrates the ability of the F-siRNA to be switched off in real time, *in vivo*. These results are a clear indication that the F-siRNA when exposed to green light remains in the *cis* position (Figure 3.14). This supports our previous work on F-siRNAs in

which they deactivated the silencing ability for up to 72 hours in HeLa cells through a 1-hour exposure to green light post transfection.[29] Unlike the prior experiments, our current model had to be re-exposed to green light after every fluorescence measurement because they were exposed to natural light when placed in the plate reader. This is still an improvement over the use of UV light with non-F-azobenzene, as visible light remains nontoxic to cells and our mammalian tissues. A future experiment could be conducted in which we expose our embryos to green light at 0 hpi for 1 hour and then keep them in complete darkness for a 72-hour period, and then measure fluorescence in order to demonstrate that the F-siRNA will remain in the off-form multiple days after injection, and the stability of the *cis* conformer in our *in-vivo* fish embryo model. This may come with additional challenges, however, as the embryo rearing solution must be changed daily to ensure the viability of the eggs and thus medium exchange would have to be completed in complete darkness.[27,33]

Regardless, exposure to 1 hour of green light immediately post injection has demonstrated the F-siRNA does not cause gene silencing for at least 24 hpi by remaining in the *cis* conformer. This inactivation demonstrates control levels of eGFP fluorescence which is what to expect when looking for a poor silencing profile.[29] Based on our previous work this is the intended result. Maintaining the inactive form of the F-siRNA for 24 hours with nominal exposure would make for a good therapeutic medication as more time in the *cis* conformer would help to control off-target effects.

3.6 Reactivation of F-siRNA with a green to blue light treatment

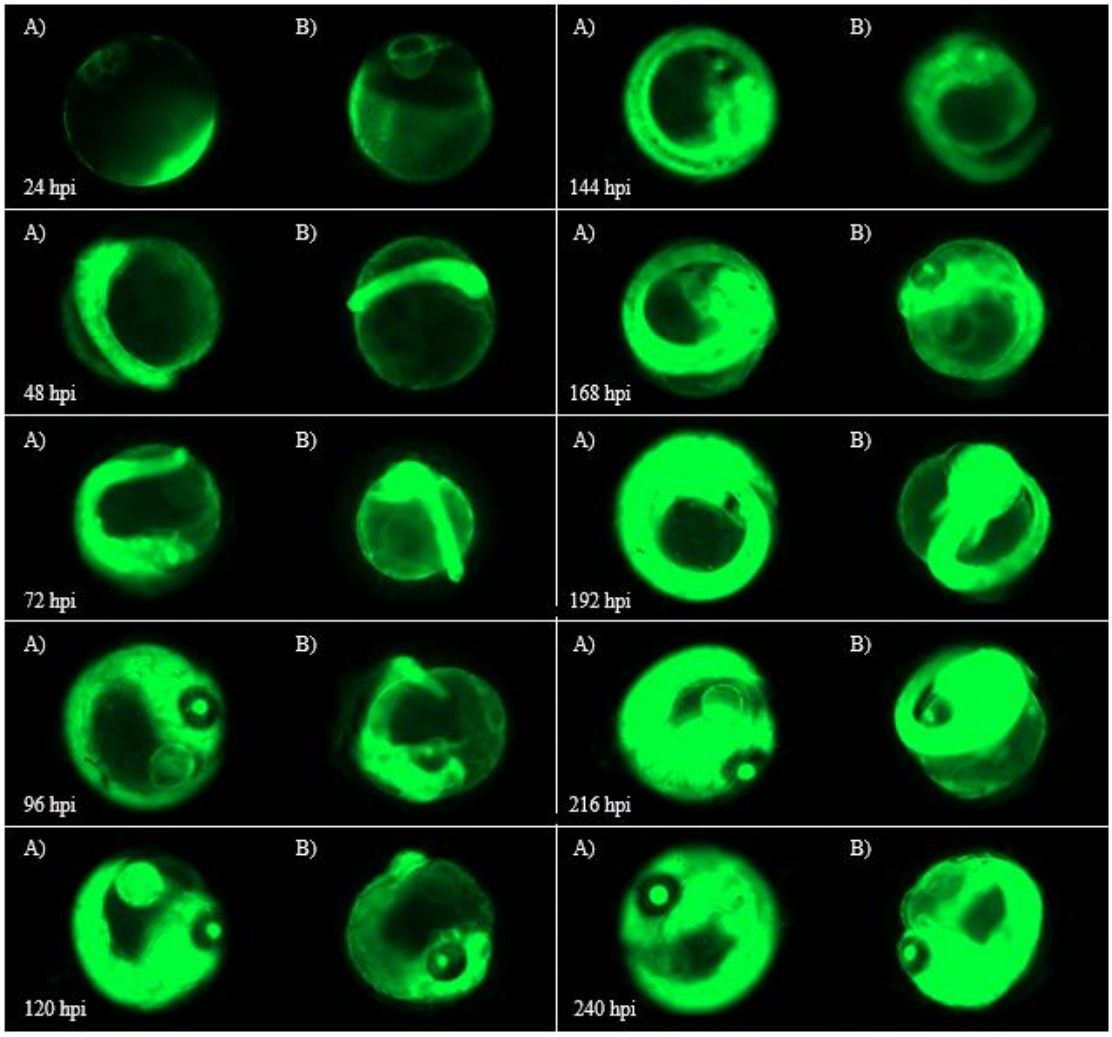

Figure 3.15 – A) Images of control Japanese Medaka embryos vs B) embryos injected with 8ng of F-siRNA-G1 held under green light for 1 hour at 0 hpi, 24 hpi, and 48 hpi then at 72 hpi held under blue light every 24 until the 240 hpi time point. (Azo G/B @72)

To ensure the F-siRNA can be reactivated from the inactive *cis* state, the embryos were given a blue light treatment after confirming siRNA inactivation. **Figure 3.15** clearly indicates where the green colour of the medaka becomes muted when compared to the control at 120 and 144 hpi. This is different from what occurred with our previous work in HeLa Cells where strong silencing was demonstrated 24 hours after flipping the azobenzene switch.[29] Both the graphical and visual data seem to emphasize that it takes at

least 48 hours post blue light activation for the results to be fully realized in a living embryo. This may be due to the nature of the embryo's growth period during the 72 to 96 hpf, and the additional complexity of a multi-cellular tissue-differentiated organism as compared to a monoculture of identical cells, as suggested earlier. The massive development could result in increased eGFP production skewing the results.[33]

Another important finding in the present study is that the F-siRNA can remain in the inactive *cis* state for at least 24 hours before being photochemically reversed to the active *trans* conformer. This result supports what was previously found in HeLa cells; however, being able to control gene silencing *in-vivo* is a new and novel development.[29] This is important as we had some uncertainty that the visible light would bypass the medaka chorion effectively enough to turn the F-siRNA on or off at the 72-hour time point. As well, as the medaka matures in the embryo, they develop many distinct cell types for protection including stratified epithelial cells, fibroblasts, melanophores, mast cells, and Merkel cells.[41,42] However, a study in 2020 determined that when exposed to large amounts of high intensity visible light for prolonged periods of time medaka embryos sustain minimal damage from oxidative stress.[42] Along with the data from the present study, this suggests our F-siRNA was hit with at least a small amount of visible light photons needed to reactivate gene silencing, and therefore bypassed some of the protective layers that incase the embryo.

Overall, the present study clearly demonstrates that reversible gene silencing can be achieved after exposure to green light through blue light. Unlike our previous work in HeLa cells, the F-siRNA cannot reach the silencing levels of the Azo Dark experiment.[29] However, this may be accounted for as the RNAi system in zebrafish fish has been shown

to be less effective due to an Ago-2 mutation resulting in impaired mRNA catalyzation.[43] It is possible this mutation is carried over to other teleost fish; however, this impairment may not be present in medaka at all. Instead, another explanation may simply be due to the half-life of the eGFP being 26 hours and the long duration of the experiment compounded with the fact that this is a novel silencing mechanism in a complex multicellular organism.[37]

3.7 Deactivation of F-siRNA with a blue to green light treatment

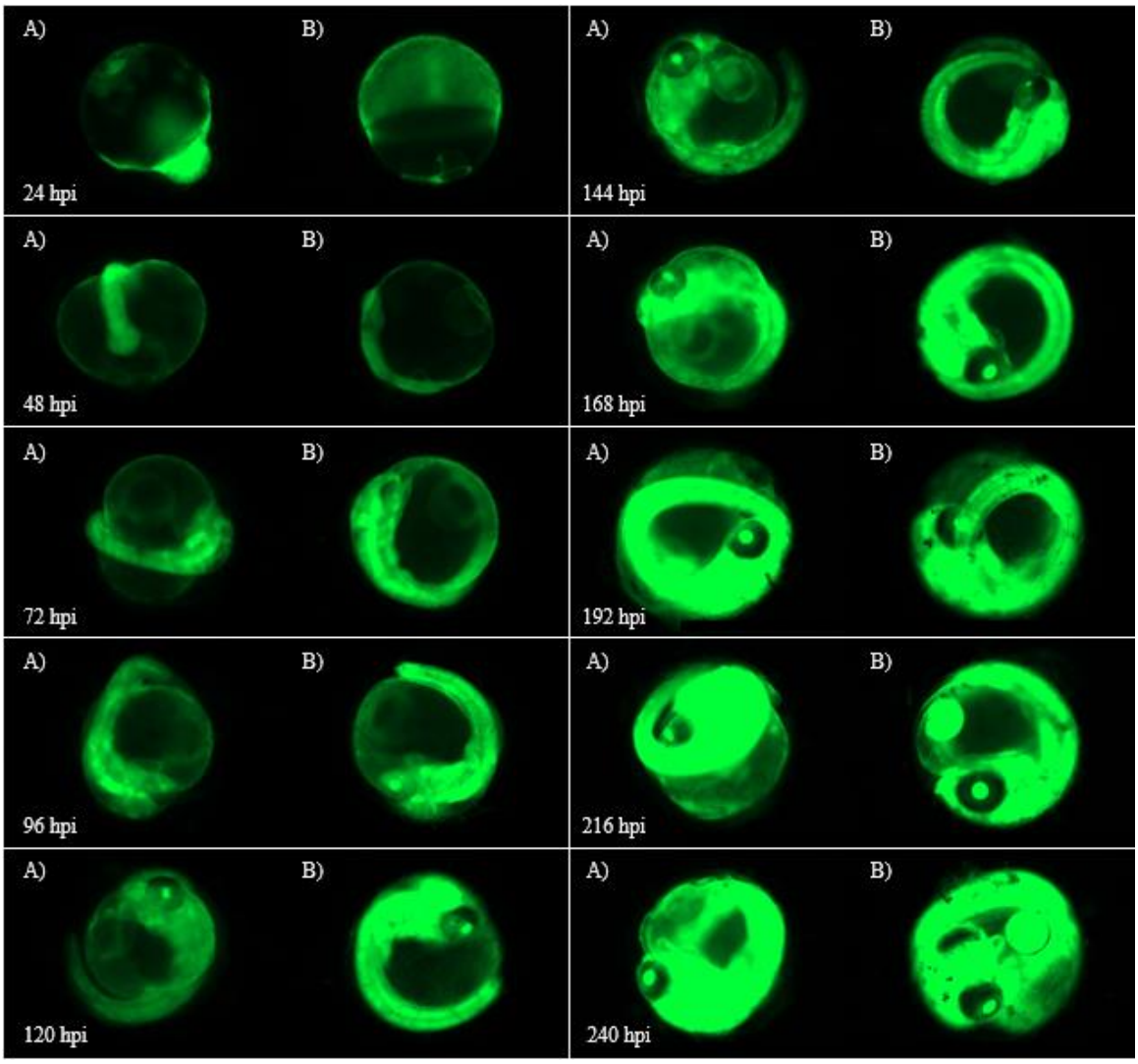

Figure 3.16 – A) Images of Azo Dark embryos vs B) embryos injected with 8ng of F-siRNA-G1 held under blue light for 1 hour at 0 hpi, 24 hpi, and 48 hpi then at 72 hpi held under green light every 24 until the 240 hpi time point. (Azo B/G @72)

To ensure the F-siRNA can be deactivated after being switched on through exposure to blue light, the embryos were given a green light treatment for 1 hour after confirming siRNA inactivation, which is evident in **Figure 3.16** where the eGFP does not decrease after 72 hpi when compared to our Azo Dark experiment where silencing took place. This is the expected result as it was our intention to stop the silencing capabilities of the F-siRNA after showing gene suppression. Overall, this is important as it demonstrates

the reversibility from the active to the inactive state for F-siRNAs in our fish embryos. This is a similar result to what we have reported earlier in HeLa cells; however, previously we never started with a blue light exposure.[29] This additional blue light exposure to start is significant as it demonstrates two new concepts. First, the F-siRNA can be exposed *in vivo* to blue light so that it is in the active state, and then it can still be switched back to the inactive state with green light, *in vivo*, which has never before been done. Instead, in earlier experiments green light would be used first and then blue light would be used. The reason for starting with blue light in our fish model system, as opposed to starting with green, and then to blue, and back to green, was due to the fact that we thought it may take time for the results to be fully realized. Notably, the inactivation of the F-siRNA (Azo B/G @72) showed quicker significant results, after 24 hours, than reactivating the F-siRNA (Azo G/B @72), after 48 hours. Due to the *trans* state being the more thermodynamically favourable state it was assumed the opposite should be the case. The second novel development is that this experiment was now conducted using fish embryos, a more complex system than HeLa cells.[29] This is consequential as it shows that the photochemical switch can be activated in vertebrates, which makes this F-SiRNA study more relevant to humans.[44] As the end goal of F-siRNAs is to potentially have them work as gene silencing therapeutics it is important to demonstrate this reversibility in complex living tissues.

3.8 Scramble control

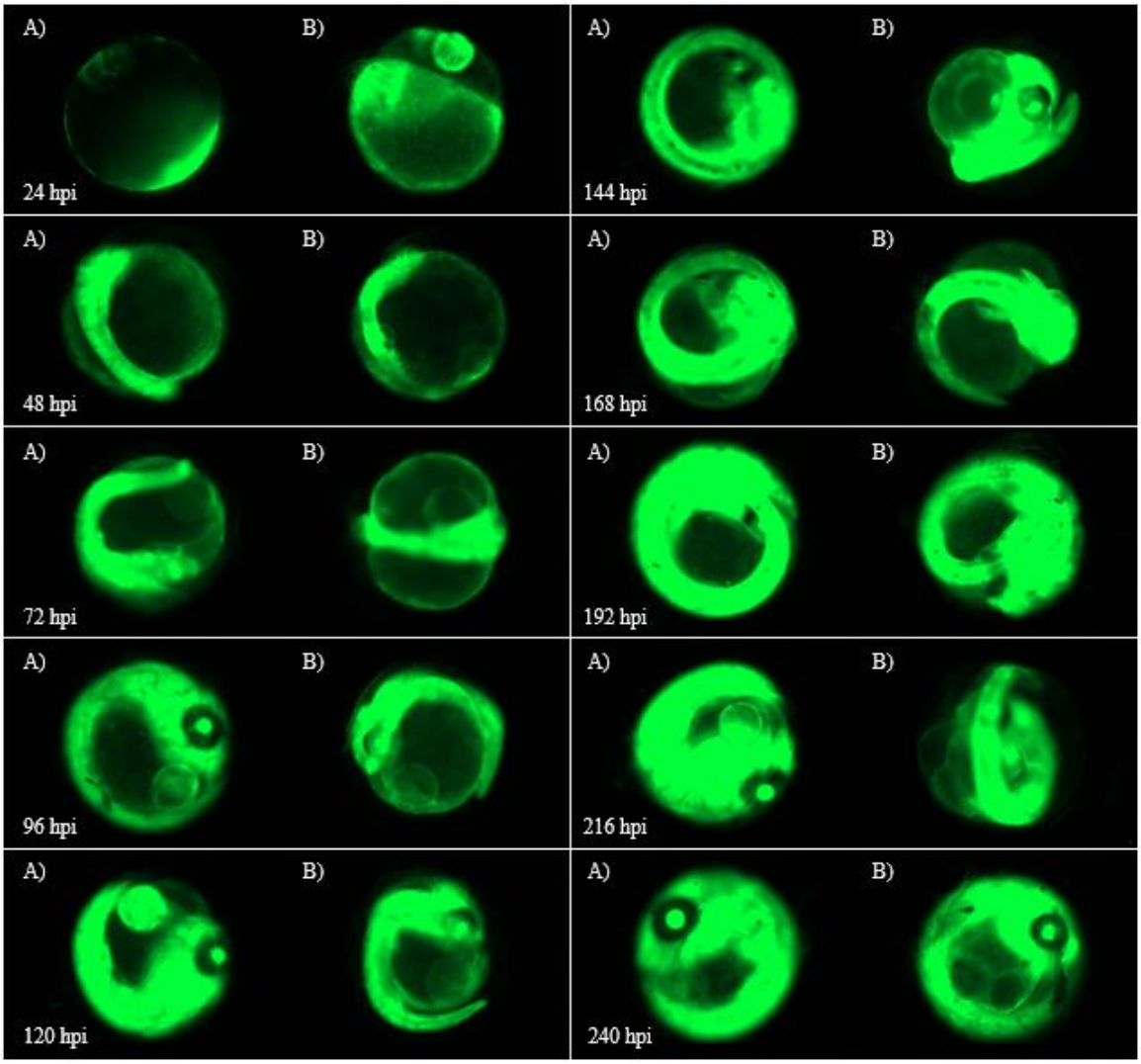

Figure 3.17 – A) Images of control Japanese Medaka embryos vs B) embryos injected with 8ng of SCR-F-siRNA-G2 h eld in the dark.

The scramble controls were used as a negative control to show injection of F-siRNA does not cause silencing through any unknown mechanism. Each time a scramble control was injected into the embryos they were subjected to the same light experiments as the F-siRNA injected embryos. **Figure 3.17** above demonstrates that the scramble control embryos given the Azo Dark treatment expressed control levels of fluorescence; and this was the case for all other treatments (data not shown).

3.9 Photoswitch mechanism

The current mechanism for this system is still unknown at the moment; however, we have two hypothesized mechanisms. The first, and more likely, mechanism is that when loaded into RISC the enzyme complex is disrupted as the F-siRNA distorts creating a bulge when in the *cis* conformer. Thus, F-siRNA annealing to its target mRNA is inhibited leading to a downregulation in silencing activity. When exposed to blue light the F-siRNA reforms to its natural conformation within the RISC complex allowing for mRNA base pairing and silencing to occur. This allows for true reversibility of the F-siRNA as the light-switching F-azobenzene modification is placed on the antisense strand and thus is retained in the RISC complex after the sense strand is discarded.

The second mechanism would occur outside of the RISC complex wherein the F-siRNA cannot be picked up by RISC when in the *cis* state and only once reverted to the *trans* state can it be loading into RISC. Once complexed the F-siRNA may not be able to revert from one state to another. This is still a plausible mechanism as we have previously before shown the azobenzene inactivation of gene silencing works when the moiety is on the sense strand.[45] After transfection only about 4% of active siRNA is immediately bound into the RISC complex, as such, it is possible the system prevents uptake of the remaining unbound siRNA into RISC.[46]

One thing of note is the long-lasting effects of the siRNA despite there being no modifications to stabilize the siRNA. Not much is known about the production of RNases in the early medaka embryo and as such it is possible these RNA degrading enzymes are sparce during early embryonic development. To test this theory a western blot targeting nucleases' can be conducted every 24 hpf going to 144 hpf. From the silencing data we

obtained our hypothesis would be as time goes on an increase in nuclease presence should appear, with minimal accumulation at 24 hpf and potentially around 120 hpf a saturation.

Chapter 4: Conclusion and Future work

4.1 Conclusions

The present study explored as proof of concept, the photochemical control of F-siRNA activity in live Tg Japanese medaka embryos by using only visible light. To do this a variety of light experiments were implemented, including: a full green light exposure to demonstrate how the F-siRNA remains inactive when exposed to 530 nm wavelength light; a green light to blue light experiment where the siRNA was inactivated and then exposed to 470 nm blue wavelength light re-activate silencing; and finally, the reverse of was carried out (blue to green light) to show how the F-siRNA can be deactivated from the active state. This represents a significant advancement upon our previous systems wherein the need for UV light has been eliminated, the half-life of the inactive *cis* conformer is longer, and the tunable control of gene silencing has been demonstrated in a live embryo. To our knowledge, this is the first time an siRNA with an azobenzene moiety has been used to reversibly control gene silencing in a fish embryo system. This is a dramatic step forward by showing the physiological relevance of our novel F-siRNA in a complex, multicellular system. Overall, this is one step closer to being able to one day use these modified azobenzene siRNAs for therapeutic use, helping to counteract any off-target effects current oligonucleotide medications may cause. Moreover, siRNA toxicity may also be diminished due to the *cis* form being stable for up to 24 hour which when inactive should not affect other biological functions. In fact, treatments could be conducted at home as all that is required to photoswitch is minimal light exposure after injection. In conclusion, this

technology has the potential to be revolutionary in gene therapeutics for both quality-of-life improvements of treatment and eliminating current siRNA challenges.

4.2 Future work

The light experiment tests conducted in this study were designed to demonstrate the robustness of the F-siRNA to activate and deactivate gene silencing in living organisms. To further expand upon these, ON/OFF cycling tests could be conducted in which the embryos are first exposed to green light at time 0 hpi, then blue light at 24 hpi, and finally green light again at 72 hpi. The fluorescent measurements taken at 96 hpi should show minimal eGFP silencing, which would further demonstrate the reversibility of our F-siRNA. This experiment could be taken further by adding in a final blue light treatment which may show silencing again. However, it is suspected, due to the nature of naked siRNA being degraded quickly, that past the 72 hpi time point a photoswitch will not work.[47] This experiment can then be reconducted in reverse. At time 0 hpi blue light would be exposed to the embryos, then at 16 hpi green light, then finally at 24 hpi blue light again. The eGFP fluorescence measurement should be taken around 72 hpi to gage if silencing is occurring due to the 48-hour time period it took to see silencing in our study. Moreover, to further demonstrate the results of this study RT-qPCR analysis can be conducted on the eggs to show silencing of the F-siRNA.

Moving on from medaka it may be useful to test this system in other organisms, such as rainbow trout. In fact, the first effective siRNA knockdown system conducted in fish was done using rainbow trout to silence GFP. Due to the larger size of the fish, it may be possible to test the F-siRNA in just the eyes, demonstrating proof of concept for our future ocular therapeutic. This could entail purchasing a rainbow trout that express eGFP

in the eyes and then administering the F-siRNA in a safe and effective manner such that it could silence our intended target. Visible blue or green light can be safely exposed to the eye and then at a later time expression of the target gene can be measured through RT-qPCR or perhaps even fluorescence readings if possible.

BIBLIOGRAPHY

(1) Watts, J. K.; Corey, D. R.. Silencing Disease Genes in the Laboratory and the Clinic. *The Journal of Pathology* **2012**, *226* (2), 365–379. https://doi.org/10.1002/path.2993.

(2) Ahn, I.; Kang, C. S.; Han, J.. Where Should Sirnas Go: Applicable Organs for Sirna Drugs. *Experimental & Molecular Medicine* **2023**, *55* (7), 1283–1292. https://doi.org/10.1038/s12276-023-00998-y.

(3) Sajid, M. I.; Moazzam, M.; Kato, S.; Yeseom Cho, K.; Tiwari, R. K.. Overcoming Barriers for Sirna Therapeutics: From Bench to Bedside. *Pharmaceuticals* **2020**, *13* (10), 294. https://doi.org/10.3390/ph13100294.

(4) Ali Zaidi, S. S.; Fatima, F.; Ali Zaidi, S. A.; Zhou, D.; Deng, W.; Liu, S.. Engineering Sirna Therapeutics: Challenges and Strategies. *Journal of Nanobiotechnology* **2023**, *21* (1). https://doi.org/10.1186/s12951-023-02147-z.

(5) Petri, S.; Dueck, A.; Lehmann, G.; Putz, N.; Rüdel, S.; Kremmer, E.; Meister, G. Increased siRNA duplex stability correlates with reduced off-target and elevated on-target effects. *Rna* **2011**, *17* (4), 737-749. DOI: 10.1261/rna.2348111 From NLM.

(6) Padda, I. S.; Mahtani, A. U.; Parmar, M. Small Interfering RNA (siRNA) Therapy. In *StatPearls* **2023**, StatPearls Publishing LLC., 2023.

(7) Springer, A. D.; Dowdy, S. F.. Galnac-sirna Conjugates: Leading the Way for Delivery of Rnai Therapeutics. *Nucleic Acid Therapeutics* **2018**, *28* (3), 109–118. https://doi.org/10.1089/nat.2018.0736.

(8) Vutrisiran. In *LiverTox: Clinical and Research Information on Drug-Induced Liver Injury*, National Institute of Diabetes and Digestive and Kidney Diseases, 2012.

(9) Keam, S. J.. Vutrisiran: First Approval. *Drugs* **2022**, *82* (13), 1419–1425. https://doi.org/10.1007/s40265-022-01765-5.

(10) Gavrilov, K.; Saltzman, W. M. Therapeutic siRNA: principles, challenges, and strategies. *Yale J Biol Med* **2012**, *85* (2), 187-200.

(11) Bechhofer, D. H.; Deutscher, M. P.. Bacterial Ribonucleases and Their Roles in RNA Metabolism. *Critical Reviews in Biochemistry and Molecular Biology* **2019**, *54* (3), 242–300. https://doi.org/10.1080/10409238.2019.1651816.

(12) Sajid, M. I.; Moazzam, M.; Kato, S.; Yeseom Cho, K.; Tiwari, R. K.. Overcoming Barriers for Sirna Therapeutics: From Bench to Bedside. *Pharmaceuticals* **2020**, *13* (10), 294. https://doi.org/10.3390/ph13100294.

(13) Bartlett, D. W.. Insights into the Kinetics of Sirna-mediated Gene Silencing from Live-cell and Live-animal Bioluminescent Imaging. *Nucleic Acids Research* **2006**, *34* (1), 322–333. https://doi.org/10.1093/nar/gkj439.

(14) Dana, H.; Chalbatani, G. M.; Mahmoodzadeh, H.; Karimloo, R.; Rezaiean, O.; Moradzadeh, A.; Mehmandoost, N.; Moazzen, F.; Mazraeh, A.; Marmari, V.; et al. Molecular Mechanisms and Biological Functions of siRNA. *Int J Biomed Sci* **2017**, *13* (2), 48-57.

(15) Sudbery, I.; Enright, A. J.; Fraser, A. G.; Dunham, I.. Systematic Analysis of Off-target Effects in an Rnai Screen Reveals Micrornas Affecting Sensitivity to Trail-induced Apoptosis. *BMC Genomics* **2010**, *11* (1), 175. https://doi.org/10.1186/1471-2164-11-175.

(16) Zlatev, I.; Castoreno, A.; Brown, C. R.; Qin, J.; Waldron, S.; Schlegel, M. K.; Degaonkar, R.; Shulga-Morskaya, S.; Xu, H.; Gupta, S.; Matsuda, S.; Akinc, A.; Rajeev, K. G.; Manoharan, M.; Maier, M. A.; Jadhav, V.. Reversal of Sirna-mediated Gene Silencing in Vivo. *Nature Biotechnology* **2018**, *36* (6), 509–511. https://doi.org/10.1038/nbt.4136.

(17) Selvam, C.; Mutisya, D.; Prakash, S.; Ranganna, K.; Thilagavathi, R.. Therapeutic Potential of Chemically Modified Sirna: Recent Trends. *Chemical Biology & Drug Design* **2017**, *90* (5), 665–678. https://doi.org/10.1111/cbdd.12993.

(18) Kaushal, A.. Innate Immune Regulations and Various Sirna Modalities. *Drug Delivery and Translational Research* **2023**, *13* (11), 2704–2718. https://doi.org/10.1007/s13346-023-01361-4.

(19) Ly, S.; Echeverria, D.; Sousa, J.; Khvorova, A.. Single-stranded Phosphorothioated Regions Enhance Cellular Uptake of Cholesterol-conjugated Sirna but Not Silencing Efficacy. *Molecular Therapy - Nucleic Acids* **2020**, *21*, 991–1005. https://doi.org/10.1016/j.omtn.2020.07.029.

(20) Hall, A. H.; Wan, J.; Shaughnessy, E. E.; Ramsay Shaw, B.; Alexander, K. A. RNA interference using boranophosphate siRNAs: structure-activity relationships. *Nucleic Acids Res* **2004**, *32* (20), 5991-6000. DOI: 10.1093/nar/gkh936

(21) Wu, S. Y.; Chen, T. M.; Gmeiner, W. H.; Chu, E.; Schmitz, J. C. Development of modified siRNA molecules incorporating 5-fluoro-2'-deoxyuridine residues to enhance cytotoxicity. *Nucleic Acids Res* **2013**, *41* (8), 4650-4659. DOI: 10.1093/nar/gkt120

(22) Kwiatkowska, A.; Sobczak, M.; Mikolajczyk, B.; Janczak, S.; Olejniczak, A. B.; Sochacki, M.; Lesnikowski, Z. J.; Nawrot, B. siRNAs modified with boron cluster and their physicochemical and biological characterization. *Bioconjug Chem* **2013**, *24* (6), 1017-1026. DOI: 10.1021/bc400059y

(23) Hartley, G. S.. The Cis-form of Azobenzene. *Nature* **1937**, *140* (3537), 281–281. https://doi.org/10.1038/140281a0.

(24) Tait, K. M. Parkinson, J. A. Bates, S. P. Ebenezer, W. J. Jones, A. C., The novel use of NMR spectroscopy with in situ laser irradiation to study azo photoisomerization. *Journal of Photochemistry and Photobiology a-Chemistry* **2003,** *154* (2-3), 179-188.

(25) Yamana, K.; Kan, K.; Nakano, H. Synthesis of oligonucleotides containing a new azobenzene fragment with efficient photoisomerizability. *Bioorg Med Chem* **1999**, *7* (12), 2977-2983. DOI: 10.1016/s0968-0896(99)00244-8

(26) Rastogi, R. P.; Richa; Kumar, A.; Tyagi, M. B.; Sinha, R. P.. Molecular Mechanisms of Ultraviolet Radiation-induced DNA Damage and Repair. *Journal of Nucleic Acids* **2010**, *2010*, 1–32. https://doi.org/10.4061/2010/592980.

(27) Hammill, M. L.; Islam, G.; Desaulniers, J. P. Synthesis, Derivatization and Photochemical Control of ortho-Functionalized Tetrachlorinated Azobenzene-Modified siRNAs. *Chembiochem* **2020**, *21* (16), 2367-2372. DOI: 10.1002/cbic.202000188

(28) Sherwood, V. F.; Kennedy, S.; Zhang, H.; Purser, G. H.; Sheaff, R. J. Altered UV absorbance and cytotoxicity of chlorinated sunscreen agents. *Cutan Ocul Toxicol* **2012**, *31* (4), 273-279. DOI: 10.3109/15569527.2011.647181

(29) Hammill, M. L.; Tsubaki, K.; Wang, Y.; Islam, G.; Kitamura, M.; Okauchi, T.; Desaulniers, J. P. Synthesis, Derivatization and Photochemical Control of an ortho-Functionalized Tetrafluorinated Azobenzene-Modified siRNA. *Chembiochem* **2022**, *23* (20), e202200386. DOI: 10.1002/cbic.202200386

(30) Guzman-Aranguez, A.; Loma, P.; Pintor, J.. Small-interfering Rnas (sirnas) as a Promising Tool for Ocular Therapy. *British Journal of Pharmacology* **2013**, *170* (4), 730–747. https://doi.org/10.1111/bph.12330.

(31) Friedrich, M.; Aigner, A.. Therapeutic Sirna: State-of-the-art and Future Perspectives. *BioDrugs* **2022**, *36* (5), 549–571. https://doi.org/10.1007/s40259-022-00549-3.

(32) Tamimi, N. A. M.; Ellis, P.. Drug Development: From Concept to Marketing! *Nephron Clinical Practice* **2009**, *113* (3), c125–c131. https://doi.org/10.1159/000232592.

(33) Iwamatsu, T. Stages of normal development in the medaka Oryzias latipes. *Mech Dev* **2004**, *121* (7-8), 605-618. DOI: 10.1016/j.mod.2004.03.012

(34) Murakami, Y.; Kinoshita, M. Medaka-microinjection with an Upright Microscope. *Bio Protoc* **2018**, *8* (3), e2716. DOI: 10.21769/BioProtoc.2716

(35) Boonanuntanasarn, S.; Yoshizaki, G.; Takeuchi, T. Specific gene silencing using small interfering RNAs in fish embryos. *Biochem Biophys Res Commun* **2003**, *310* (4), 1089-1095. DOI: 10.1016/j.bbrc.2003.09.127

(36) Hosono, K.; Noda, S.; Shimizu, A.; Nakanishi, N.; Ohtsubo, M.; Shimizu, N.; Minoshima, S. YPEL5 protein of the YPEL gene family is involved in the cell cycle progression by interacting with two distinct proteins RanBPM and RanBP10. *Genomics* **2010**, *96* (2), 102-111. DOI: 10.1016/j.ygeno.2010.05.003

(37) Kitsera, N.; Khobta, A.; Epe, B.. Destabilized Green Fluorescent Protein Detects Rapid Removal of Transcription Blocks After Genotoxic Exposure. *BioTechniques* **2007**, *43* (2), 222–227. https://doi.org/10.2144/000112479.

(38) Tschuch, C.; Schulz, A.; Pscherer, A.; Werft, W.; Benner, A.; Hotz-Wagenblatt, A.; Barrionuevo, L.; Lichter, P.; Mertens, D.. Off-target Effects of Sirna Specific for GFP. *BMC Molecular Biology* **2008**, *9* (1), 60. https://doi.org/10.1186/1471-2199-9-60.

(39) Ishigaki, M.; Yasui, Y.; Puangchit, P.; Kawasaki, S.; Ozaki, Y.. In Vivo Monitoring of the Growth of Fertilized Eggs of Medaka Fish (oryzias Latipes) by Near-infrared Spectroscopy and Near-infrared Imaging—a Marked Change in the Relative Content of Weakly Hydrogen-bonded Water in Egg Yolk Just Before Hatching. *Molecules* **2016**, *21* (8), 1003. https://doi.org/10.3390/molecules21081003.

(40) Pratt, A. J.; Macrae, I. J.. The Rna-induced Silencing Complex: A Versatile Gene-silencing Machine. *Journal of Biological Chemistry* **2009**, *284* (27), 17897–17901. https://doi.org/10.1074/jbc.r900012200.

(41) Le Guellec, D.; Morvan-Dubois, G.; Sire, J.-Y.. Skin Development in Bony Fish with Particular Emphasis on Collagen Deposition in the Dermis of the Zebrafish (danio Rerio).. *The International Journal of Developmental Biology* **2004**, *48* (2-3), 217–231. https://doi.org/10.1387/ijdb.15272388.

(42) Merino, M.; Mullor, J.; Sánchez-Sánchez, A.. Medaka (oryzias Latipes) Embryo as a Model for the Screening of Compounds That Counteract the Damage Induced by Ultraviolet and High-energy Visible Light. *International Journal of Molecular Sciences* **2020**, *21* (16), 5769. https://doi.org/10.3390/ijms21165769.

(43) Chen, G. R.; Sive, H.; Bartel, D. P.. A Seed Mismatch Enhances Argonaute2-catalyzed Cleavage and Partially Rescues Severely Impaired Cleavage Found in Fish. *Molecular Cell* **2017**, *68* (6), 1095–1107.e5. https://doi.org/10.1016/j.molcel.2017.11.032.

(44) Mattes, W. B. In Vitro to in Vivo Translation. *Current Opinion in Toxicology* **2020**, *23–24*, 114–118. https://doi.org/10.1016/j.cotox.2020.09.001.

(45) Hammill, M. L.; Isaacs-Trépanier, C.; Desaulniers, J.-P. siRNAzos: A New Class of Azobenzene-Containing siRNAs that Can Photochemically Regulate Gene Expression. *ChemistrySelect* **2017**, *2* (30), 9810-9814. DOI: https://doi.org/10.1002/slct.201702322.

(46) Addepalli, H.; Meena; Peng, C. G.; Wang, G.; Fan, Y.; Charisse, K.; Jayaprakash, K. N.; Rajeev, K. G.; Pandey, R. K.; Lavine, G.; et al. Modulation of thermal stability can enhance the potency of siRNA. *Nucleic Acids Res* **2010**, *38* (20), 7320-7331. DOI: 10.1093/nar/gkq568

(47) Bartlett, D. W.. Insights into the Kinetics of Sirna-mediated Gene Silencing from Live-cell and Live-animal Bioluminescent Imaging. *Nucleic Acids Research* **2006**, *34* (1), 322–333. https://doi.org/10.1093/nar/gkj439.

APPENDICES

A1. ^{1}H NMR spectra

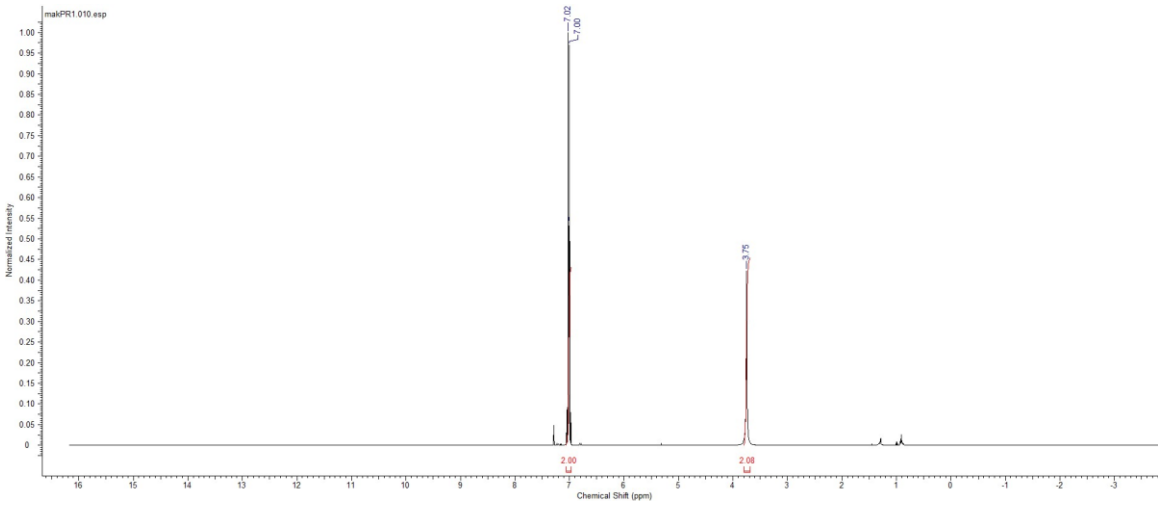

A1.1. ^{1}H NMR Spectrum **4-bromo-2,6-difluoroaniline** Compound (**2**) in $CDCL_3$ at 400 MHz.

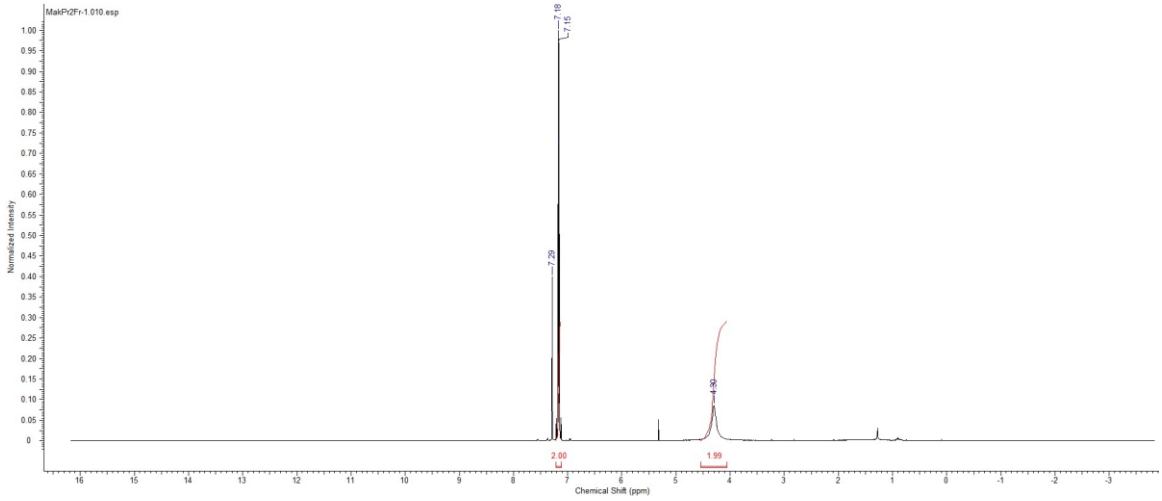

A1.2. ^{1}H NMR Spectrum **4-amino-3,5-difluorobenzonitrile** Compound (**3**) in $CDCL_3$ at 400 MHz.

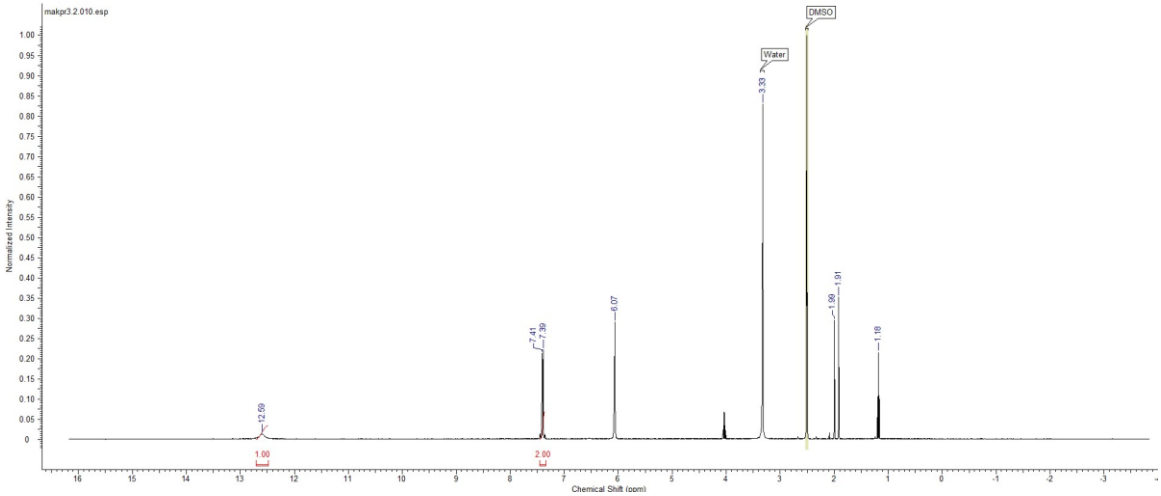

A1.3. ^{1}H NMR Spectrum **4-amino-3,5-difluorobenzoic acid** Compound (**4**) in DMSO-d_6 at 400 MHz.

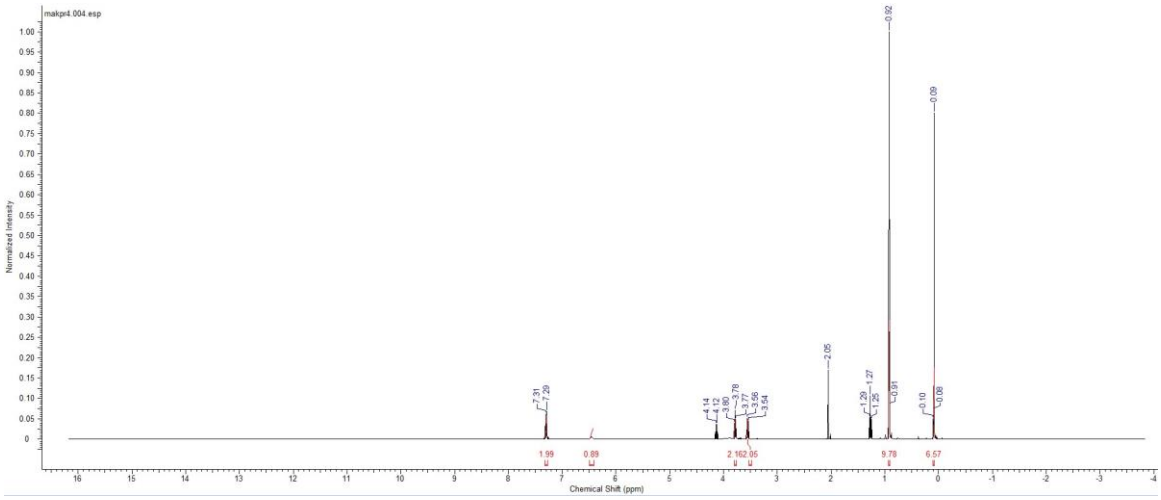

A1.4. ^{1}H NMR Spectrum **4-amino-N-(2-((tert-butyldimethylsilyl)oxy)ethyl)-3,5-difluorobenzamide** Compound (**5**) in $CDCL_3$ at 400 MHz.

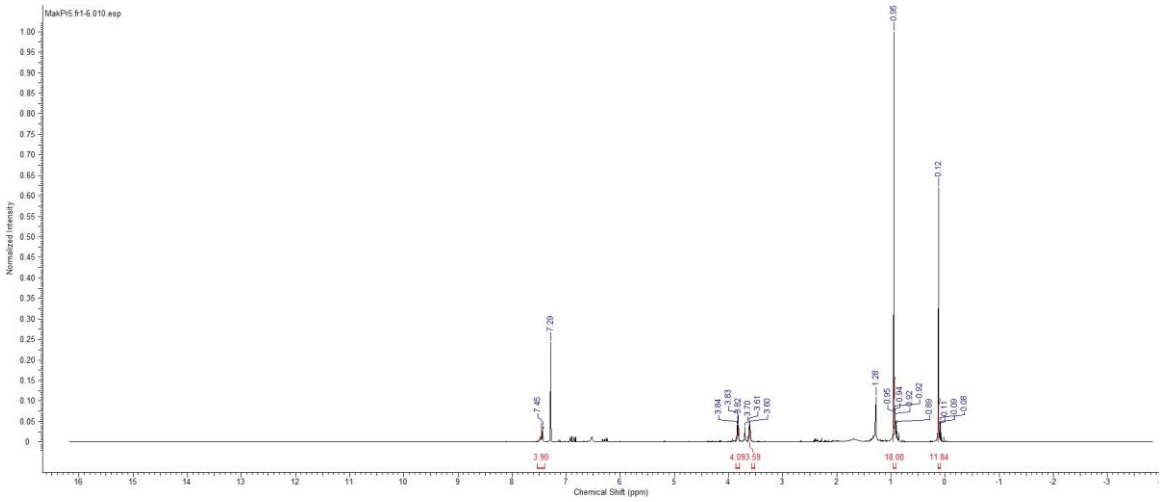

A1.5. ^{1}H NMR Spectrum (**E)-4,4'-(diazene-1,2-diyl)bis(N-(2-((tert-butyldimethylsilyl)oxy)ethyl)-3,5- difluorobenzamide (**Compound (**6**) in $CDCL_3$ at 400 MHz.

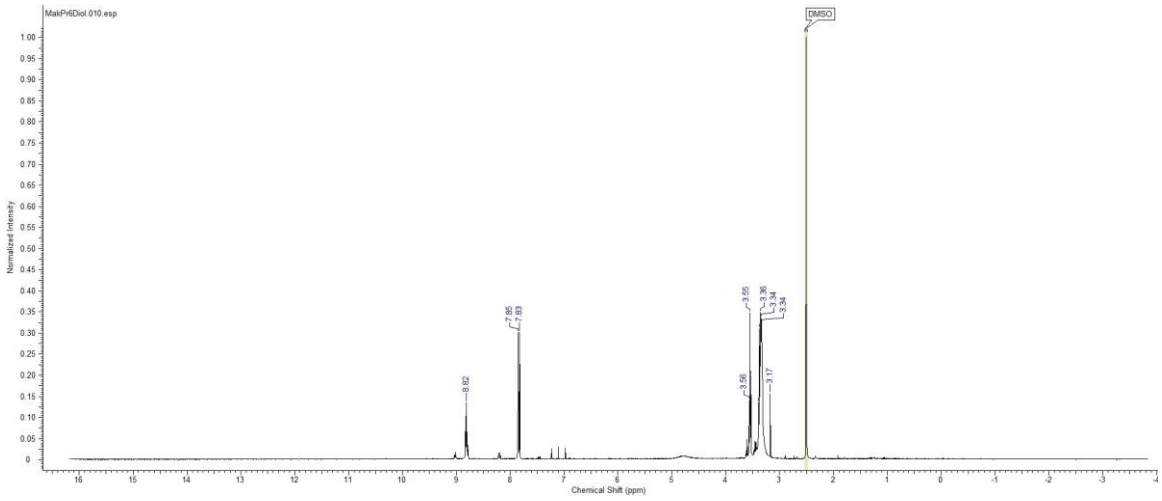

A1.6. ^{1}H NMR Spectrum **(E)-4,4'-(diazene-1,2-diyl)bis(3,5-difluoro-N-(2-hydroxyethyl)benzamide)** Compound (**7**) in DMSO-d_6 at 400 MHz.

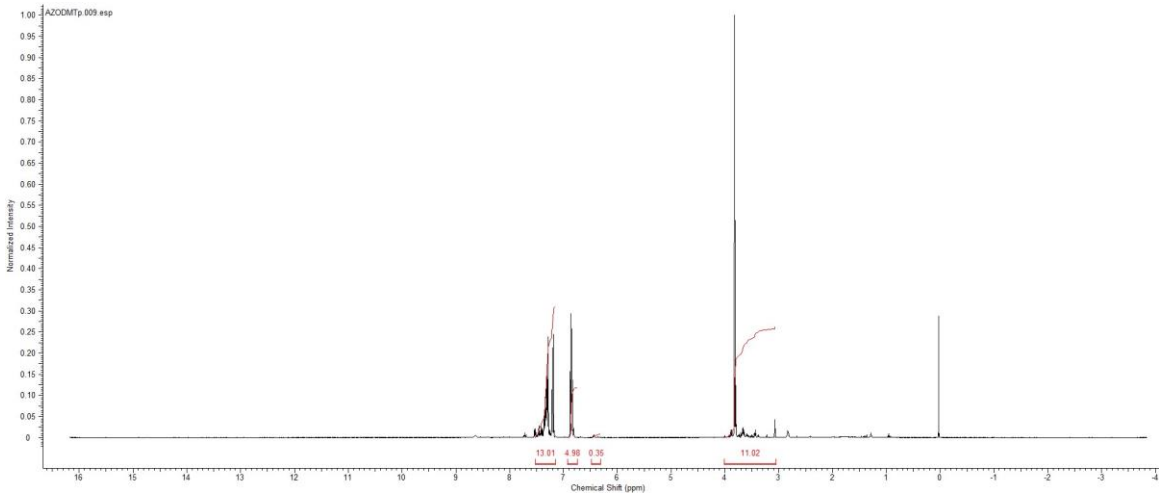

A1.7. ^{1}H NMR Spectrum **(E)-N-(2-(bis(4-methoxyphenyl)(phenyl)methoxy)ethyl)-4-((2,6-difluoro-4-((2-hydroxyethyl)carbamoyl)phenyl)diazenyl)-3,5difluorobenzamide** Compound (**8**) in $CDCL_3$ at 400 MHz.

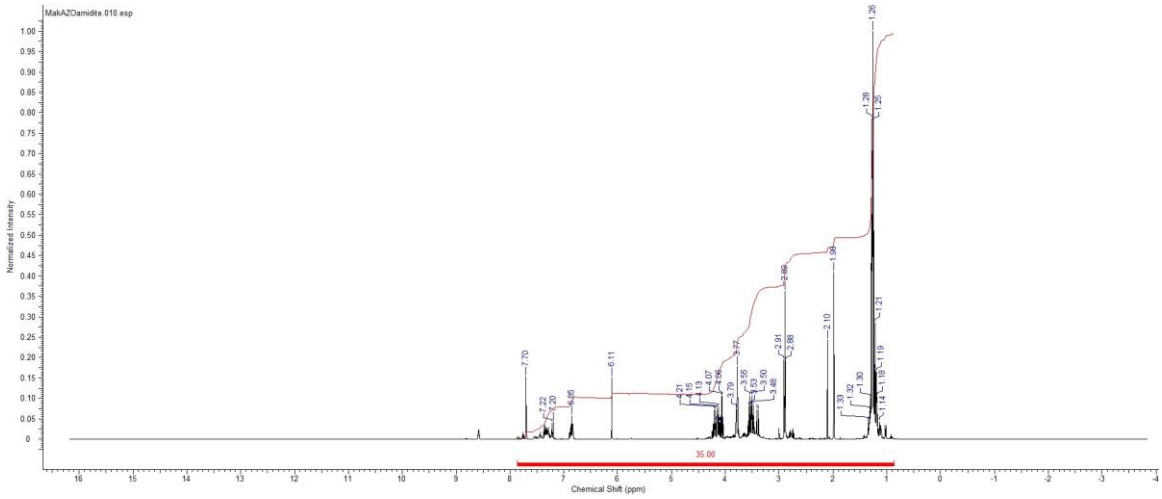

A1.8. ^{1}H NMR Spectrum **(E)-2-(4-((4-((2-(bis(4-methoxyphenyl)(phenyl) methoxy)ethyl)carbamoyl)-2,6-difluorophenyl)diazenyl)-3,5difluorobenzamido)ethyl (2-cyanoethyl) diisopropylphosphoramidite** Compound (**9**) in $CDCL_3$ at 400 MHz.

A2. CD spectra

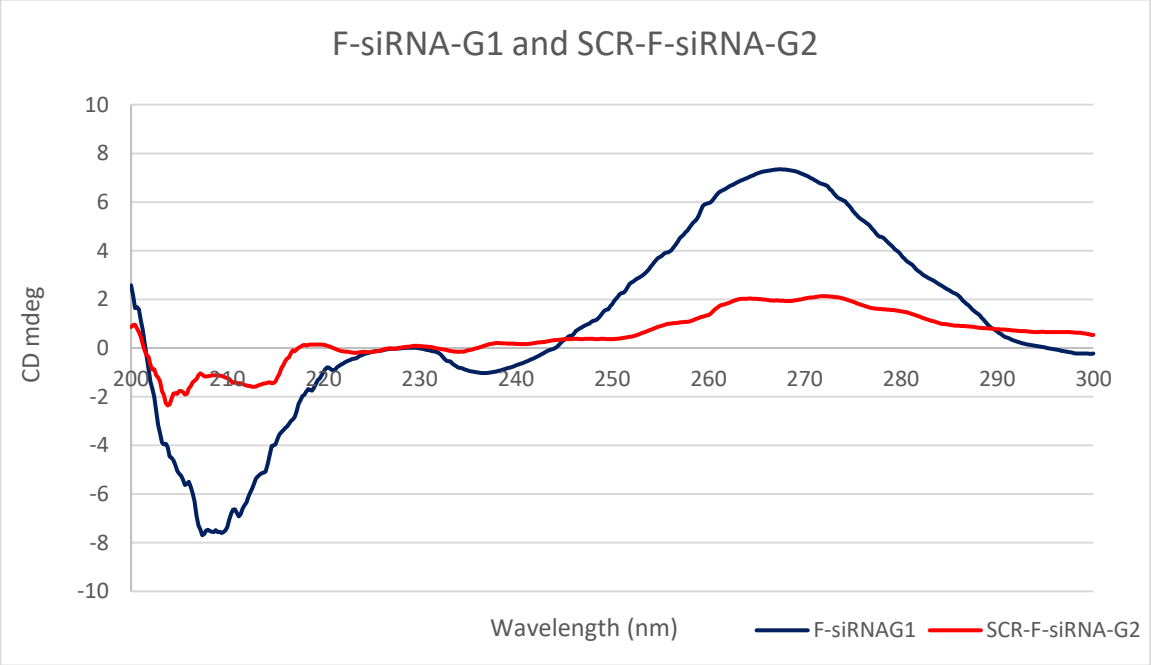

A2.1 CD spectra of azobenzene modified spacers replacing two nucleobases targeting eGFP mRNAs. All scans were performed in triplicate and averaged using Jasco's Spectra Manager version.

A3. HPLC

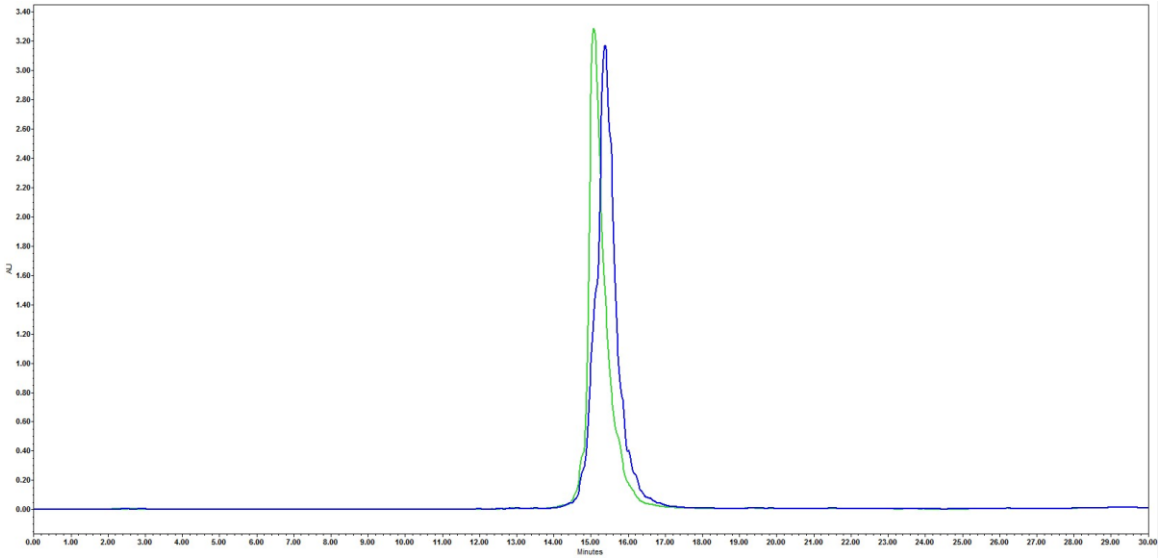

A3.1. HPLC chromatogram for the antisense strand of F-siRNA-G1 in the *trans* conformer (blue) and the *cis* conformer (green). To ensure the strand was in the *trans* conformer the experiment was conducted in the dark with only 470nm blue light being exposed to the F-siRNA strand. This was repeated for the *cis* conformer using 530nm green light.

A4. LC/MS Spectra

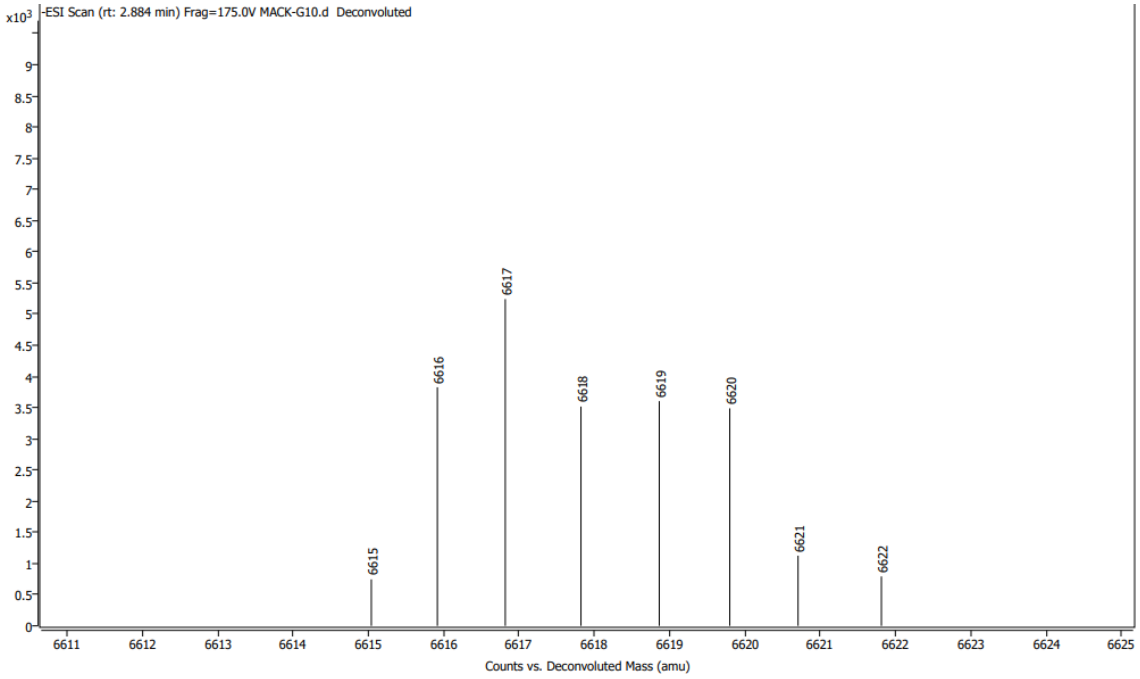

A4.1. LC/MS chromatogram for the antisense strand of F-siRNA-G1 in the *trans* conformer.

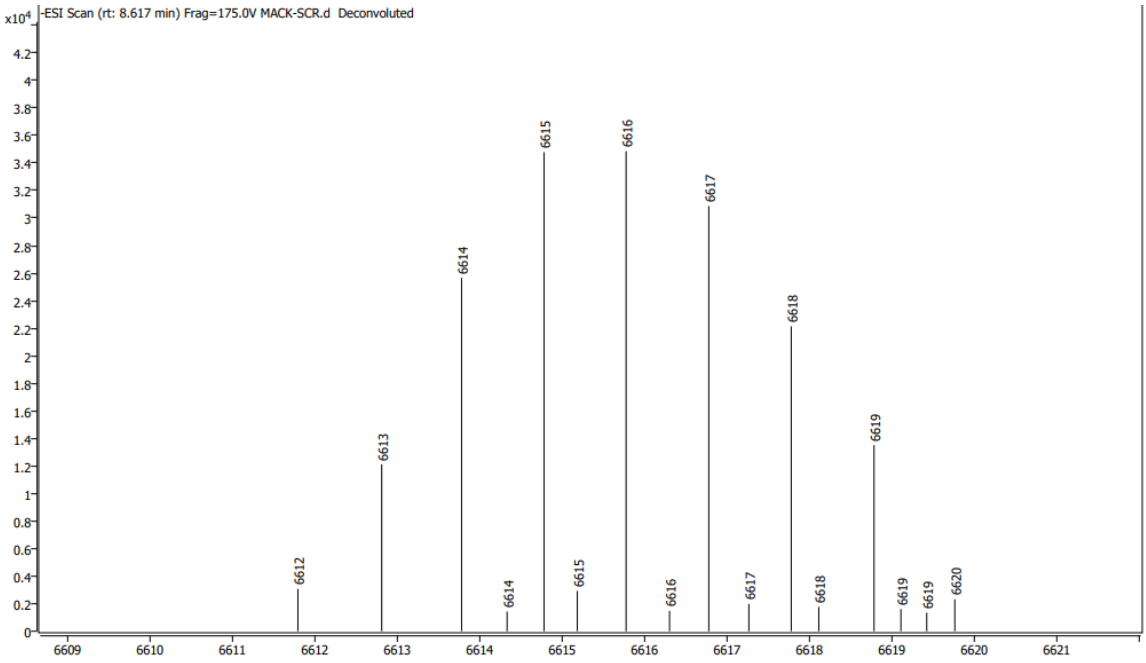

A4.2. LC/MS chromatogram for the antisense strand of SCR-F-siRNA-G2 in the *trans* conformer.